

The Regional Specialization Trade-off

Lukas Boehnert*
University of Oxford

Job Market Paper
[[Most recent version here](#)]

October 13, 2025

Abstract

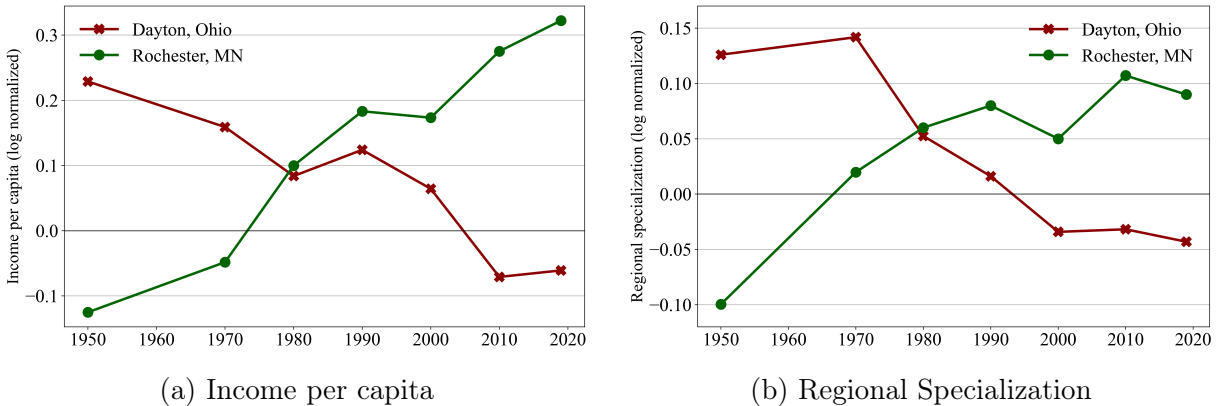
I document a specialization trade-off in U.S. regional growth. In 1950, regions specialized into particular industries had higher per capita income than those with greater diversity. Since then, however, the more specialized regions have grown persistently slower. I formalize this trade-off in a dynamic multi-industry model featuring two opposing forces. First, specialization raises productivity and income through agglomeration economies. Second, it increases exposure to sectoral shocks. Real factor adjustment costs and financial frictions make reallocation in response to shocks costly and long-lasting. A quantitative version of the model, disciplined by U.S. Census data, reveals that financial frictions account for roughly half of the adverse effect of specialization on regional growth. A constrained-efficient planner balances the agglomeration and frictions when allocating factors, and highlights the potential for optimal industrial policy.

*University of Oxford, Department of Economics, Email: lukas.boehnert@economics.ox.ac.uk. I am thankful to Federica Romei and Todd Schoellman for their support and guidance. I am also grateful to Andrea Chiavari, Andrea Ferrero, Sergio de Ferra, Fabrizio Perri, and Petr Sedlacek for the helpful comments and discussions.

1 Introduction

The economic fortunes of regions can shift dramatically over time. Once-thriving hubs often face long-term decline, while other areas rise to prominence. This paper offers new evidence that a crucial factor in explaining regional variation is the degree of *regional specialization* — the concentration of economic activity in a few specific industries. While economic theory often frames specialization as a benefit of comparative advantage, this paper argues it is a double-edged sword: the industrial structure that makes a region prosperous in the short run can make it vulnerable to steep and lasting declines in the long-run.¹

I begin by documenting three novel facts about U.S. regional growth using U.S. Census microdata. First, commuting zones (henceforth, regions) that were more specialized in 1950 had higher per capita incomes than more diversified regions. Since then, however, these specialized regions have exhibited persistently lower long-run growth. This highlights a *specialization trade-off* where regions benefit from focusing resources on a specific industry today but may be persistently worse off when this industry declines in the future. Second, as regions grow, they become more specialized (and vice versa). Third, the specialization at the region-industry level, however, is highly persistent. Once a region is specialized in one industry, it tends to maintain this specialization in the long-run.



(a) Income per capita

(b) Regional Specialization

Figure 1: The specialization trade-off: Historical example

Notes: Panel (1a) shows the relative log per capita income of the Dayton, Ohio and Rochester Minnesota commuting zones relative to the rest of the U.S. since 1950. Panel (1b) shows the relative regional specialization of the two regions. Specialization is measured as the Gini coefficient on income shares across 3-digit Census industries. Further detail on the measure is provided in section (2).

As an example of these facts, consider the divergent economic trajectories of Dayton, Ohio, and Rochester, Minnesota as shown in Figure (1). Dayton's economy was once dominated by a single industry - the manufacturing of cash registers, led by the National Cash Register

¹For a summary of specialization benefits, see e.g. Costinot, Donaldson, et al. (2015).

company (NCR). While this specialization initially brought prosperity, the city's fortunes were dependent on this one sector. When technological change and global competition led to NCR's decline, Dayton's lack of industrial diversity resulted in a prolonged economic descent, leaving a legacy of idle manufacturing plants.

Rochester's development provides a stark contrast. Alongside its mid-century manufacturing base, anchored by an IBM facility, the city fostered a robust healthcare sector centered on the renowned Mayo Clinic. This economic diversity proved critical. When the manufacturing sector declined, the expanding Mayo Clinic provided a new engine for growth. Unlike Dayton, Rochester successfully transitioned its economy, becoming one of the nation's wealthiest mid-size metropolitan areas.

Motivated by these novel empirical facts, this paper examines how regional specialization affects growth and what degree of specialization is optimal. To address these questions, I develop a dynamic multi-sector model that links specialization to growth and formalizes a trade-off between benefits and costs of specialization. In the model, specialization increases productivity and income through industry-specific agglomeration forces. In line with a vast existing literature, these forces capture the *benefits of specialization* (as in e.g., Bartelme et al. (2019)). The model's key contribution is then to endogenize the *costs of specialization* by showing how it can lead to persistently lower long-run growth. These costs arise through two dynamic frictions. First, adjustment costs make reallocating factors after shocks an inherently slow and costly process. Second, a financial friction in the form of an occasionally binding collateral constraint amplifies and propagates adverse shocks, especially for highly specialized regions.² Together, these frictions imply that specialization not only increases exposure to industry-specific shocks but also increases the cost of responding to them. For specialized regions this can create "lock-in" effect, where a region's economic trajectory becomes tied to the fate of its dominant industry.

I then calibrate the model using U.S. Census data on all 722 commuting zones and use the calibrated model to derive two quantitative results.³ First, I apply the model to understand U.S. regional growth since 1950. Matching the initial relative income and specialization of all commuting zones and simulating forward using realized industry productivity paths, the model is able to capture 51% of the relationship between relative specialization in 1950 and 1950-2020 income growth across the U.S..

Second, the calibrated model attributes an important role to financial amplification in explaining the persistence of regional specialization and heterogeneity in growth. When a region becomes financially constrained following a transitory, adverse sectoral shock, the

²Well-known examples of similar financial amplification include Kiyotaki and Moore (1997) and Bianchi and Mendoza (2018)

³I take the geographical definition of commuting zones from Dorn (2009).

reallocation of capital across industries is almost halved in the medium term. Intuitively, hitting the collateral constraint limits the amount of financing available for new investment and thereby suppresses the ability to re-specialize the economy. A counterfactual simulation exercise in which a region is not subject to the financial friction shows that 56% of the effect of specialization on growth stem from the financial amplification mechanism. Over seven decades, convex adjustment costs alone generate only a quarter of the persistence and amplification of shocks necessary to match the observed regional specialization.

Next, I employ the model to address the second key question of this paper: What is the optimal degree of regional specialization given that future growth across industries is uncertain? To address this, I derive the optimal specialization implemented by a constrained-efficient, regional planner. Two counteracting sources of inefficiencies motivate the planner to deviate from the decentralized, competitive equilibrium allocation. First, the agglomeration externality incentivizes the planner to increase the specialization of a region. This agglomeration effect captures within-industry knowledge and productivity spillovers that increase with industry size and are not internalized by private agents.

The second inefficiency stems from the risk of specialization captured by the occasionally binding collateral constraint. The constraint takes physical capital valued at its market price as collateral. While private agents takes this price as given when allocating capital across industries, the planner internalizes the effect of her decisions on the current and future price of capital - the pecuniary externality. I extend the results from standard financial amplification models (Kiyotaki and Moore, 1997; Bianchi and Mendoza, 2018) to a multi-industry setting to show that the responsiveness of the capital price to an industry-specific productivity shock increases with the degree of regional specialization. The risk of becoming financially constrained therefore incentivizes the planner to diversify a region.⁴ Intuitively, the planner understands that by being more diversified across industries, an industry-specific shock moves the price of capital by less. As the price of capital determines the tightness of the collateral constraint, a more diversified economy is thereby less likely to become constrained and to enter a vicious downturn.

With these two opposing forces, the optimal degree of specialization becomes a quantitative question. I return to the calibrated model to estimate the socially optimal specialization and measure the welfare difference between the decentralized competitive equilibrium and the constrained-efficient planner equilibrium. The analysis shows that for some regions, the planner increases specialization, as the agglomeration benefits outweigh the risk of industry-specific shocks. Conversely, for others, the planner chooses to diversify when the costs of shock exposure are the dominant concern. The model reveals that the industrial

⁴In addition, the planner saves more relative to the private agent as is standard in financial amplification models Bianchi (2011).

composition implemented by a regional planner in 1950 would raise welfare by 1.2 to 2.2 percent depending on the commuting zone. Finally, I show that the planner can implement the optimal specialization using a combination of state-contingent industry taxes and subsidies and a state-contingent tax on debt.⁵

Related literature.

I contribute to three strands of literature. The first one is the regional growth literature that links regional growth to structural change at the national level (see, e.g. Barro and Sala-i-Martin (1992), Autor, Katz, and Kearney (2008), Autor, Dorn, et al. (2020), and Eckert and Peters (2022)), trade liberalization (Caliendo, Dvorkin, and Parro (2019), Allen and Arkolakis (2014), and Fajgelbaum and Redding (2022)), misallocation (Fajgelbaum, Morales, et al., 2019; Ganong and Shoag, 2017), employment (Autor, Patterson, and Van Reenen, 2023; Bilal, 2023), innovation (Desmet and Rossi-Hansberg, 2014) and start-up location (Walsh, 2023). Building on this, my primary contribution is to identify and formalize a specialization trade-off in U.S. regional growth. The trade-off demonstrates that the nature of regional economic structure is another important mediating factor of regional convergence.

The notion of specialization trade-offs can be traced back to seminal work by Jacobs (1969), Jacobs (1985), and Glaeser et al. (1992). More recently, Hebllich et al. (2025) have documented a similar effect for cities in 19th-century Great Britain. While the authors identify a 'Jacobs externality' through which industrial concentration reduces long-run growth irrespective of industry-specific productivity trends, my model shows that this negative effect can also be understood through an asymmetric amplification channel. Specifically, I show that financial frictions induce a penalty for specialization only during adverse shocks, thereby lowering expected growth in highly specialized regions. The mechanism thus provides a novel microfoundation for the long-run costs of specialization.

Second, this paper contributes to the international trade literature by re-evaluating the long-run consequences of specialization. A large amount of trade literature portrays specialization according to comparative advantage as a source of welfare gains (Costinot and Donaldson, 2012; Costinot, Donaldson, et al., 2015; Moroney and Walker, 1966). While some studies acknowledge adjustment costs in the short run (Caselli et al., 2020), the long-run benefits of specialization are rarely questioned. I contribute to this field by showing that while specialization can raise short-term efficiency through agglomeration economies (Bartelme et al., 2019; Moretti, 2010; Walsh, 2023), it can also create path dependencies that are detrimental to long-run growth, offering a theoretical and empirical counterpoint.

⁵The planner will also choose a lower level of bond holdings as is standard in the financial amplification literature.

Finally, to capture the risk of the trade-off, I introduce a financial amplification channel, building on the literature on local financial frictions and growth. This work typically examines how shocks are amplified and can lead to financial crises and sudden stops (Kiyotaki and Moore, 1997; Bernanke, Gertler, and Gilchrist, 1999; Gertler and Karadi, 2011; Mendoza, 2010). My model extends this research by showing how a region's degree of specialization can interact with financial conditions. Specifically, I extend Bianchi and Mendoza (2018) to a multi-industry setting showing how specialized regions may attract concentrated investment in the short run but become more exposed to financial downturns in response to industry-specific shocks in the long run.

The rest of the paper is structured as follows. Section (2) provides the empirical evidence. Section (3) introduces the model and section (4) the quantitative analysis. The constrained-efficient quantitative results are discussed in section (5). Finally, section (6) concludes.

2 Empirical Analysis

I document three novel facts about US regional growth since 1950. Together, these facts show that the degree of industrial specialization of regions plays a significant role in determining current income and long-run income growth. Throughout the paper, I will use commuting zones (CZ) as the primary geographic unit which I also refer to interchangeably as a region.

Data. I assemble data from three main sources. First, I collect nationally representative sample of individual-level data from the decennial US Census. The survey is run every ten years between 1950 and 2010. After 2010, I supplement the Census dataset with the Consumer Population Survey (CPS) together with its Annual Social and Economic Supplement (ASEC). Both cover information on a range of economic, employment, demographics topics including income measures and information on the region of residence. I assign individuals to one of 741 mutually exclusive and exhaustive local labor markets that correspond to commuting zones defined by Dorn (2009). While many papers in the spatial economics literature focus on pre-defined Metropolitan Statistics Areas (MSAs), using commuting zones provides two key advantages. First, a commuting zone is the most precise way of defining a local labor market. In the analysis that follows, the definition of a local labor market is crucial as it implies that agents cannot move across markets free of costs and non-tradable prices are defined locally. In contrast, there is no reason why a local labor market should be bounded by county or even state-level borders. Second, the commuting zones used are mutually exclusively covering all of the US. Instead, MSA only cover the

largest economic areas leaving some regions undocumented.

Second, I use aggregate data at the county-industry level US for employment, population and GDP across all industries since 1950 from the County Business Patterns (CBP) as well as data on the firm population from the Business Dynamics Statistics (BDS) since 1978. Since the classification of industries changed from SIC to NAICS in 1998, I use the crosswalk from Eckert, Fort, et al. (2020) to match industries over time.

Finally, data on housing and land units as values as types and values are obtained from the decennial county-level sample of the US Housing Census. The Housing Census runs since 1970 which restricts part of my analysis to the last 50 years.

Measuring specialization. Specialization refers to the concentration of economic activity across industries. Following Imbs and Wacziarg (2003), I focus on the Gini coefficient for the inequality of industry shares as the main measure of specialization: the more equal industry shares, the more diversified the economy. A Gini coefficient of 1 implies maximum specialization with all value generated within one industry. The baseline measure of industry shares will be pre-tax wage and salary income generated by the working age population (age 25-60) at the 3-digit CPS industry level defined in 1990.⁶ In defining this measure, I follow Heathcote, Perri, Violante, and L. Zhang (2023) and adjust top-coded income variables in line with the literature.⁷ I run the replacement of top-coded values on state-level rather than US-level income distribution as explained in further detail in Appendix (A.1). I use the US Census 3-digit industry classification which implies 946 industries at the most granular level. For part of the analysis, I aggregate income shares up to 9 aggregate industries in line with the NAICS classification. A detailed list of industry details can be found in Appendix (A.2).

Fact 1: *Highly specialized regions are richer in the short-run but have lower long-run growth.*

Figure (2) presents the specialization trade-off: Highly specialized regions are richer in the short-run but experience lower growth in the long-run. It shows the residualized linear fit between current income (left) and long-run growth (right) and initial industrial specialization after controls. I estimate this effect across US CZs with the following regression:

$$Y_c = \alpha + \beta \cdot Gini_{c,1950} + \delta \cdot \hat{g}_c + \gamma' \cdot Z_{c,1950} + \epsilon_c \quad (1)$$

where Y_c is the dependent variable for CZ c and $Gini_{c,1950}$ is the measure of industrial

⁶Appendix (A.3) shows that the results are robust to choosing value added of employment shares as variables of other indexes (e.g. HHI or max share) as measures for specialization.

⁷Further studies I follow are Moffitt and S. Zhang (2018) and Heathcote, Perri, and Violante (2010).

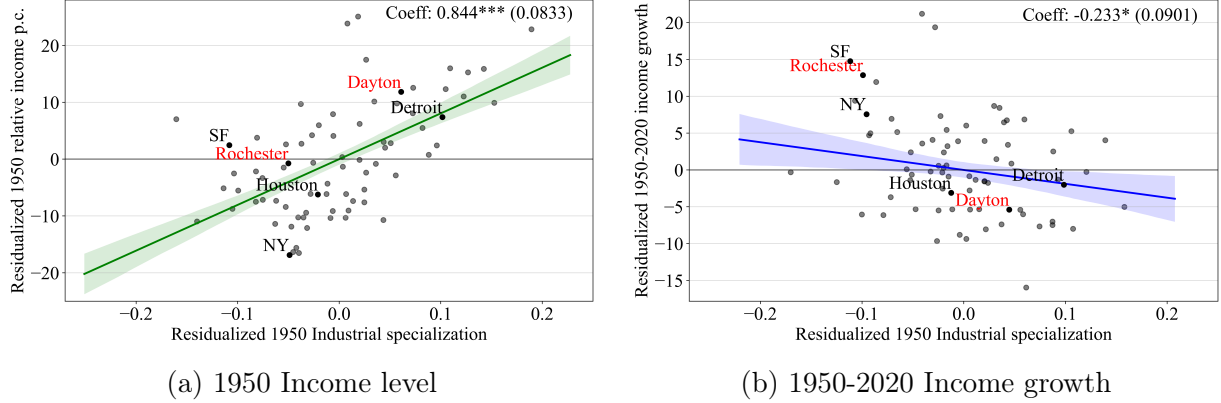


Figure 2: The specialization trade-off after controls

Notes: Figure (2) shows the residualized linear fit from regression (5) for 1950 per capita income level (2a) and 1950-2020 per capita income growth (2b). Specialization is measured as the Gini coefficient of income shares across 3-digit 1990 US Census industries. 95% Confidence intervals are shaded.

specialization by 3-digit industry. I augment the regression with two sets of controls. First, I control for the exposure to structural change across sectors at the 1-digit NAICS level (e.g. agriculture, manufacturing or services) that gave rise to winners and losers across US regions. In order to assess the impact of industrial specialization beyond the direct impact of structural change, I follow Borusyak, Hull, and Jaravel (2025) in using a shift-share instrument to isolate the effect of industrial composition. Specifically, I compute the exposure to structural change by including the predicted growth across industries based on a region's initial share in these industries as follows:

$$\hat{g}_c = \sum_{i=1}^I s_{i,c} \cdot g_i \quad (2)$$

where $s_{i,c}$ is the regions 1950 income share and g_i is the 1950-2020 aggregate income growth of industry i . Thus \hat{g}_c captures the predicted growth of region c given its initial exposure to aggregate changes across industries. The coefficient β can then be interpreted as the effect of specialization on relative income after controlling for exposure to aggregate changes across industries and production structure over time.

The second set of controls $Z_{c,1950}$ includes the 1950 per capita income, population size, share of high-skilled workers, old-age dependency ratio, share of female workers in logs as well as a dummy for whether the CZ is located within the rustbelt. All of these controls are introduced to capture well-known confounding forces that drive growth between 1950-2020 and may directly relate to the industrial composition of a region.⁸

⁸Initial income levels capture possible convergence (or catch-up) forces often observed in regional growth (see e.g. Eckert (2019)).

The regression shows that a one standard deviation rise in specialization in 1950, implies a $2/3$ of a standard deviation rise in 1950 relative income and a $1/3$ of a standard deviation fall in the long-run. The regression table including all controls can be found in Appendix (A.3).

Robustness and Extensions. I run a range of robustness and extension exercises on the regression defined above. First, it is important to note that the time horizon matters for the relationship between specialization and growth. In the baseline, I choose to define long-run growth over the longest horizon possible given the data to show that specialization matters has a long-lasting impact. In addition, I also run regression (5) over shorter time horizons as shown in Appendix (A.3). The results suggest that a negative growth impact of specialization becomes evident over a 20-year horizon already. The analysis over different time horizons, however, is limited by the available data. Ideally, one could assess the degree of specialization and relative growth going back to the beginning of industrialization and showcase what has led to a regions industrial specialization in 1950. While existing literature (see, e.g. Nagy (2023) and Hebllich et al. (2025)) has provided some reasoning for historical causes of specialization pre-1950, this is beyond the scope of this paper.

Second, I decompose the effect of specialization by industry and tradability. I find that virtually all of the relevance of specialization for contemporary and future relative income of labor markets is linked to specialization within tradable industries. Intuitively, whether a region is disproportionately concentrated within non-tradable industries (e.g. a city has relatively many hairdressers) matters little for relative income and long-run growth. Instead, if all of a region's tradable output is generated in a single industry (e.g. cash registers as in Dayton, Ohio) appears to significantly reduce the likelihood of sustained long-run growth. The regression results by industry and tradability can be found in Appendix (A.3).

Fact 2: *As regions grow, they become more specialized.*

The second fact is about the dynamics of regional specialization over time. Intuitively, as U.S. regions grow and move up in the income distribution, they become more specialized. And vice versa, regions that once were rich and specialized become more diversified as they decline.

In order to understand the dynamics of regional specialization I proceed in two steps. First, I summarize the evolution of regional specialization across the US over time. Table (1) shows both the average regional specialization as well as its dispersion in the U.S. since 1950 in terms of both income and employment shares. Since 1950, the U.S. has experienced a rise in regional specialization by 15%. At the same time, the dispersion of specialization

has declined by around 50%. Together, these statistics imply that the U.S. is becoming more concentrated both on aggregate and at the regional level.

Year	Income Shares			Employment Shares		
	Mean	CV	p90/p10	Mean	CV	p90/p10
	(1)	(2)	(3)	(4)	(5)	(6)
1950	0.46	0.162	1.55	0.45	0.152	1.50
1970	0.48	0.123	1.35	0.47	0.116	1.35
1990	0.47	0.089	1.23	0.46	0.082	1.26
2010	0.53	0.089	1.29	0.50	0.073	1.20
2020	0.53	0.089	1.24	0.51	0.068	1.20

Table 1: US Regional industrial specialization over time

Notes: Table (1) summarizes measures of U.S. regional specialization for Commuting Zones over time. Specialization is measured by the Gini coefficient, calculated on 3-digit industry shares of income and employment. Columns 1 and 4 report the mean specialization across zones. Columns 2 and 5 show the coefficient of variation (CV), and columns 3 and 6 show the 90/10 percentile ratio as measures of dispersion.

Next, I examine how the relative specialization of a region moves relative to the aggregate over time. I log-normalize per capita incomes and Gini coefficients. The key challenge in characterizing the dynamics of the relationship lies in its potential nonlinearity. Specifically, relative income and specialization may not move monotonically over time. In order to deal with potential nonlinearity, I follow Imbs and Wacziarg (2003) in documenting the relationship between regional sectoral concentration and the relative level of per capita income using a non-parametric locally weighted scatterplot estimation. The idea of this method is to impose as little structure on the functional form of the relationship as possible. The point estimates are computed from fitted values within weighted intervals around the independent variable from the following regression

$$y_i = \alpha(x_i) + \beta(x_i)x_i + \epsilon_i \quad (3)$$

where i corresponds to a single observation (Commuting zones - year) and x_i , y_i is the log-normalized income and the Gini coefficient, respectively.⁹ The point estimates are then given by

$$(\hat{\alpha}(x_i), \hat{\beta}(x_i)) = \arg \min_{\alpha, \beta} \sum_j w_j(x_i)(y_i - (\alpha + \beta x_j))^2 \quad (4)$$

with weights $w_j(x_i)$.¹⁰ The resulting curve of fitted values can be interpreted as the typical degree of industrial specialization for a commuting zone along the income dimension.¹¹

⁹For a more detailed explanation see Imbs and Wacziarg (2003).

¹⁰The estimation uses tricube weights. Note that rectangular or Gaussian weights give similar results.

¹¹I also run the estimation for each decade since 1950 with similar estimates across time and as a standard OLS as shown in Appendix (A.4).

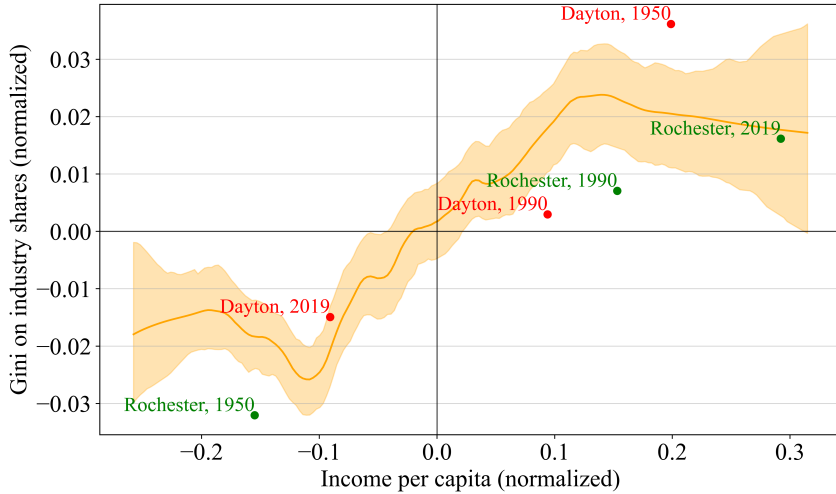


Figure 3: Non-parametric estimate: Specialization vs. per capita income

Notes: Figure (3) plots fitted values of normalized relative specialization against relative income. The line is estimated using the non-parametric regression in equation (3), with the 95% bootstrapped confidence interval shown as a shaded area. The observations for Dayton, Ohio, and Rochester, Minnesota, are highlighted.

Figure (3) shows the estimated relationship between relative per capita income and specialization since 1950: The degree of relative specialization increases with relative income along an S-shaped curve. As a region moves within the distribution of per capita incomes in the U.S. it changes its degree of relative specialization. Towards the tail ends of either distribution the relationship flattens indicating that the marginal effect of specialization on income decreases in the extremes. It is important to note, that there is no causality to this statement so it could equally be made in reverse.

Finally, the relationship of specialization and income among U.S. regions appears to differ from the relationship estimated at the cross-country level by Imbs and Wacziarg (2003). The authors find a significant U-shaped relationship where countries first become more diversified and then more specialized as they grow. In their analysis, both the poorest and wealthiest countries are the most specialized while mid-income nations are most diversified.

Fact 3: Specialization at the region-industry level is highly persistent.

This fact documents that industries in their relative importance do not move across regions over time. Intuitively, a region that was the biggest producer in a single industry in 1950 (e.g. cash registers as in Dayton, Ohio) is likely to still be the biggest producer in that industry today, irrespective of how that industry developed on the aggregate.

In order to measure the persistence of a region's relative specialization within a certain

industry, I define a region's revealed comparative advantage (RCA):

$$RCA_{i,c,t} = \frac{Y_{i,c,t}}{\sum_{i \in I} Y_{i,c,t}} / \frac{Y_{i,US,t}}{\sum_{i \in I} Y_{i,US,t}} \quad (5)$$

where $Y_{i,c,t}$ is the income generated in industry i in CZ c . In line with trade literature, the RCA measures how much more prevalent an industry is in a region relative to the US as a whole. An $RCA > 1$ implies relative specialization. I follow Morris-Levenson (2022) and rank regions based on their RCA in an industry and use this ranking in the following regression:

$$\text{logRankRCA}_{i,c,t} = \alpha + \beta_h \cdot \text{logRankRCA}_{i,c,t-h} + \delta_{c,t} + \gamma_{i,t} + \epsilon_{i,c,t}$$

where β_h is the rank-rank elasticity of the revealed comparative advantage over horizon h . I further control for CZ-year and industry-year effects to clear for any structural differences across industries and regions over time. Figure (4) shows the persistence (β) of industry rankings over time. The persistence of specialization at the region-industry level is highest among tradable industries: a 1% increase in the ranking of specializations in industry i in 1950 implies a 0.57% increase in the ranking today. Over 70 years this is a sizeable persistence of industries.¹² More detail to persistence across different industries and regions is given in Appendix (A.5).

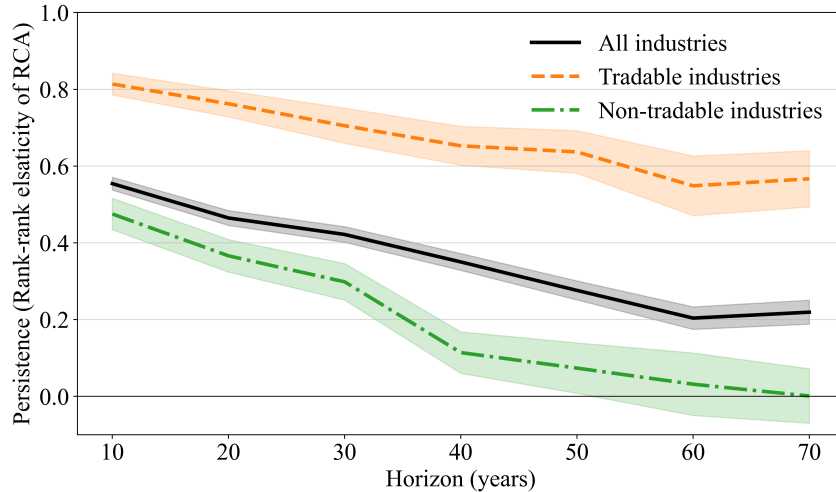


Figure 4: Persistence at the region-industry level

Notes: Figure (4) shows the rank-rank elasticity of regional revealed comparative advantage over a 70-year horizon, estimated from the regression in equation (5). The shaded area represents the 90% confidence interval. The figure also presents separate persistence estimates for tradable and non-tradable industries, as defined in Appendix (A.2).

Combined, Facts 2 and 3 suggest that once a region becomes highly specialized in a single

¹²Note that Morris-Levenson (2022) find similar estimates over even longer horizons.

industry, this specialization tends to persist over the long run, tying the region's economic trajectory to the performance of that dominant industry. While this dynamic can be advantageous for regions that happen to specialize in a high-growth sector, the historical evidence suggests that such concentration eventually exposes them to economic decline. This trade-off motivates one of the paper's central questions: What is the optimal degree of regional specialization given that future growth across industries is uncertain? In order to establish the link between specialization and growth theoretically, and to answer this question I propose a model of regional specialization in the following section.

3 A Model of Regional Specialization

In this section, I develop a dynamic multi-sector model of specialization and growth. In the model, specialization has two counteracting effects on growth that formalize a trade-off. One the one hand, it increases productivity and income through agglomeration forces. On the other hand, it makes re-specialization in response to adverse shocks costly and long-lasting through adjustment costs and a financial friction.

The goal of the calibrated model is then threefold. First, I formalize the mechanisms through which specialization affects growth. Second, I estimate the strength of the proposed mechanisms in generating specialization trade-off. Finally, I derive the optimal, constrained-efficient specialization a regional planner implements. In this section I present the model, and in the following two sections I discuss the quantitative implications.

3.1 Environment

The economy is defined as a small-open economy modeled in discrete time, indexed by t . It consists of a production side with multiple industries and a household side with a continuum of individuals.

Production and technology. Production occurs in two stages. A set of intermediate goods is produced by distinct industries, which are then aggregated to create a single final good. Each intermediate good $y_{i,t}$ is produced using capital $k_{i,t}$ in the following production function

$$y_{i,t} = z_{i,t} f(k_{i,t}) \quad (6)$$

where $z_{i,t}$ is industry-specific productivity and $f(k)$ is a twice-differentiable, concave production function. The final good output is produced by aggregating all intermediate inputs according to $Y_t = \left(\int_1^I y_{i,t}^{\frac{\sigma-1}{\sigma}} (i) di \right)^{\frac{\sigma}{\sigma-1}}$.

In this model, industries are heterogeneous along three key dimensions: productivity, capital adjustment costs and their susceptibility to agglomeration externalities. Industry-specific productivity $z_{i,t}$ is the key driver of dynamics and is assumed to follow a trend-stationary process. This captures both temporary shocks and long-run growth differences across industries. The process is defined as:

$$\bar{z}_{i,t} = \tilde{z}_i + g_{i,t}t + u_{i,t} \quad (7)$$

with log of productivity $\bar{z}_{i,t}$ defined as the sum of a linear trend $g_{i,t}$ and a stochastic shock component. The stochastic component follows a standard mean-zero AR(1) process: $u_{i,t} = \rho u_{i,t-1} + \epsilon_{i,t}$ where $\epsilon_{i,t} \sim \mathcal{N}(0, \sigma_{\epsilon_i}^2)$.

Capital accumulation in each industry is subject to idiosyncratic convex adjustment costs $\Phi_i(k_{i,t}, k_{i,t+1})$. The adjustment costs introduce persistence in the allocation of factors and represent the costs of tearing down existing machinery and plants or building new infrastructure necessary for new machinery and plants. The difference in costs across industries captures the idea that some capital may be easier to re-use for other industries. Intuitively, heavy manufacturing machinery may be more difficult to demolish than laptops used in the financial sector.

Finally, each industry is subject to an idiosyncratic agglomeration force:

$$z_{i,t} = \bar{z}_{i,t} \cdot k_{i,t}^{\xi_i} \quad (8)$$

with agglomeration parameter $\xi_i \geq 0$ captures productivity spillovers that are not internalized by private agents. In line with Bartelme et al. (2019), these externalities can arise from knowledge sharing between suppliers, a pooled market for specialized labor, or the common usage of industry-specific infrastructure.

Individuals. There is a continuum of identical, infinitely-lived individuals of measure unity with preferences given by:

$$\mathbb{E}_0 \sum_{t=0}^{\infty} \beta^t u(c_t). \quad (9)$$

Individuals in this economy operate production directly by allocating capital across all industries.¹³ They buy and sell capital from each other at the capital market price q_t . In order to invest in new capital, pay the convex adjustment costs and smooth consumption, individuals can further borrow by selling a one-period risk-free bond b_t with a world-determined gross real interest rate R_t which is taken as given.

¹³As shown by Bianchi and Mendoza (2018), the competitive equilibrium is the same if the optimization problems of households and firms are separated (assuming a frictionless equity market).

The individual's budget constraint is:

$$c_t + \frac{b_{t+1}}{R_t} + q_t \sum_{i=1}^I k_{i,t+1} = \sum_{i=1}^I [z_{i,t} f(k_{i,t}) + q_t k_{i,t} - \Phi_i(k_{i,t}, k_{i,t+1})] + b_t. \quad (10)$$

The right-hand side corresponds to the agent's income generated from production in each industry i , selling the beginning-of-period capital stock net of the adjustment costs at price q_t , and beginning-of-period bond holdings. They use this income to consume the final good c_t , buy new capital at price q_t and allocate it across industries, and save in the one-period bond. The total amount of capital is in fixed unit supply such that the market clearing condition in the capital market is simply $\sum_i k_i = 1$.

The total amount of debt individuals can borrow to invest in capital is limited by a collateral constraint.¹⁴ Debt cannot exceed a fraction θ_t of the market value of beginning-of-period asset holdings (i.e. θ_t imposes a ceiling on the leverage ratio). The market value of assets is a combination of the value of capital priced at q_t and the total amount of capital allocated across all industries i . The collateral constraint is given by:

$$-\frac{b_{t+1}}{R_t} \leq \theta_t q_t \sum_{i=1}^I k_{i,t} \quad (11)$$

The collateral constraint introduces they key financial amplification mechanism capturing the risk of specialization. It extends the results from standard incomplete financial market models (Kiyotaki and Moore, 1997; Bianchi and Mendoza, 2018) to a multi-industry setting. The motivation for this modeling choice is twofold. First, empirical evidence shows that roughly 70 percent of commercial and industrial loans are secured with collateral in the US (Gan, 2007). Second, regions hit by declines to their main industry experience rapid declines in prices and quasi defaults. Most prominent examples of this are the Rustbelt in the US with the decline of manufacturing, the Ruhrgebiet in Germany with the decline of the coal industry, or the afore-mentioned Dayton metropolitan area with a decline in cash register manufacturing.

The agent maximizes (9) subject to (10) and (11) taking prices as given. This maximization problem yields the following optimality conditions for each date $t = 0, \dots, \infty$:

$$u'(c_t)(q_t + \phi_{i,t}^2) = \beta \mathbb{E}_t [u'(c_{t+1})(q_{t+1} + z_{i,t+1} f'(k_{i,t+1}) - \phi_{i,t+1}^1) + \theta_{t+1} q_{t+1} \eta_{t+1}] \quad (12)$$

$$u'(c_t) = \beta R_t \mathbb{E}_t [u'(c_{t+1})] + \eta_t \quad (13)$$

¹⁴In line with Bianchi and Mendoza (2018) this constraint can be derived as an implication of incentive-compatibility constraints on borrowers if limited enforcement prevent lenders from collecting more than a fraction of θ_t of the asset value owned by a defaulting debtor.

where $\eta \geq 0$ denotes the Lagrange multiplier on the collateral constraint, and ϕ^s denotes the derivative of adjustment costs with respect to the s argument. The optimality conditions reveal the two key choices individuals face in this economy: A *portfolio allocation* and a *consumption vs. savings* decision.

Condition (12) presents the *portfolio allocation* choice. For each industry i , individuals allocate capital such that the marginal costs of an additional unit equate the marginal benefit. The marginal costs consist of the price of capital today and the marginal adjustment costs weighted by today's marginal utility of consumption. The marginal benefits combine the expected price at which capital can be sold next period net of adjustment costs and the expected marginal product. In addition, each unit of capital adds to the collateral value and loosens next period's collateral constraint. Note that there is only one price of capital q_t clearing the market. Intuitively, in order to sell capital on the market agents first have to turn it into marketable capital by paying the adjustment costs, and then sell it on the market at the single capital price.

The bond Euler equation (13) shows the *consumption vs. savings* decision. An unconstrained individual with $\eta = 0$ can perfectly smooth consumption across two periods by borrowing or saving in the one-period bond given the real interest rate R_t . When the collateral constraint binds, $\eta > 0$, the condition implies that the marginal benefit of borrowing exceeds the expected marginal cost by an amount equal to the shadow price of relaxing the borrowing constraint (i.e. the agent faces an effective real interest rate higher than R_t).

The existence of the occasionally binding collateral constraint introduces a wedge in the standard Euler equations. In the bond Euler equation a binding constraint today impedes consumption smoothing today. In the capital Euler equation, the expectation of a binding borrowing constraint next period raises the marginal benefit from capital.

3.2 The role of specialization

Industrial specialization in this economy has two key roles: determining the agglomeration strength, and determining the exposure to and amplification of industry-specific shocks. The impact of specialization on agglomeration is straight forward and in line with existing literature (Bartelme et al., 2019). Given a set of agglomeration parameters across industries ξ_i , a more specialized economy exhibits higher productivity and higher income per capita at every point in time.

The interaction of specialization with the price of capital and the collateral constraint in determining the exposure to and amplification of industry-specific shocks is the key novel feature of this model. The feedback loop can be summarized by in two steps. First, the

link between current specialization and the likelihood of becoming financially constrained. Second, the effect of being financially constraint on the ability to invest and adjust specialization.

Specialization and the likelihood of a crisis. The link between the current capital allocation and the likelihood of a financial crisis can be illustrated by extending standard conditions for asset pricing. First, let's define the capital share of industry i as $s_{i,t} = \frac{k_{i,t}}{\sum_i k_{i,t}}$. Industrial specialization of the economy is the concentration of economic activity across industries. In line with the definition of Imbs and Wacziarg (2003), I define specialization as the Gini coefficient on industry shares:

$$\omega_t = Gini(s_{i,t}). \quad (14)$$

The aggregate, weighted dividend (marginal product of capital net of adjustment costs) can be derived as:

$$\bar{d}_t = \sum_i s_{i,t} (z_{i,t+1} f'(k_{i,t+1}) - \phi_{i,t+1}^1) \quad (15)$$

Re-writing the definition of asset returns in aggregate terms $R_{t+1}^{\text{agg}} = \frac{q_{t+1} + \bar{d}_t}{q_t + \bar{\phi}_t^2}$, I express the pricing condition (16) as the expected present value of dividends discounted with R_{t+1}^{agg} :

$$q_t = \mathbb{E}_t \sum_{j=0}^{\infty} \left(\prod_{s=0}^j \mathbb{E}_{t+s} [R_{t+1+s}^{\text{agg}}] \right)^{-1} \bar{d}_{t+j+1} - \bar{\phi}_t^2 \quad (16)$$

where $\bar{\phi}_t^2 = \sum_i s_{i,t} \phi_{i,t}^2$ are today's weighted aggregate adjustment costs.¹⁵ Equation (16) shows that the price of capital today depends on the current and expected allocation of capital s_i , the size of adjustment costs Φ_i , and the industry-specific productivity shocks z_i . The co-movement between current capital allocation and the price of capital can be highlighted by considering three illustrative cases:

1. *Standard incomplete markets model ($I = 1$, No adjustment costs):* With only one industry and no adjustment costs, the model collapsed to the standard incomplete markets model (Kiyotaki and Moore, 1997; Mendoza, 2010). In this case, the price of capital is determined only by the dividends of the single industry.
2. *Diversification with many industries ($I > 1$, No adjustment costs):* With many industries and no adjustment costs, the co-movement of the asset price and idiosyncratic productivity shocks tends to zero, and the price of capital to unity:

¹⁵Likewise, the pricing condition can also be written as $q_t = \mathbb{E} \sum_{j=0}^{\infty} \beta^j \frac{u'(c_{t+j})}{u'(c_t)} \bar{d}_{t+j+1} - \mathbb{E} \sum_{j=0}^{\infty} \beta^j \frac{u'(c_{t+j})}{u'(c_t)} \bar{\phi}_t^2$.

$\lim_{I \rightarrow \infty} Cov(q, z_i) = 0$. All idiosyncratic risk is diversified away as capital can freely be moved across industries.

3. *Specialization matters ($I > 1$, Positive adjustment costs)*: With many industries and positive adjustment costs, the current capital allocation matters for the co-movement of the capital price and industry-specific shocks: $Cov(q, z_i) = F(s_i)$. In this case, the price of capital is determined by the current and expected allocation of capital across industries.

The third case illustrates the relevant key relationship in this paper: The more diversified an economy, the less the exposed it is to industry-specific productivity shocks and the less its price of capital co-moves with single industries. This extends the standard incomplete market model (Mendoza, 2010) to a multi-industry setting. The above mechanism is at the core of the model's pecuniary externality.

The collateral constraint and the ability to invest. Now consider the second part of the feedback loop: the interaction between the collateral constraint and specialization. To study the relationship, I re-write the bond Euler equation as:

$$R_t \beta^j \mathbb{E}_t \left[\frac{u'(c_{t+j})}{u'(c_t)} \right] = R_t \mathcal{M}_{t,t+j} = (1 - \eta_t) \quad (17)$$

where $\mathcal{M}_{t,t+j}$ denotes the stochastic discount factor (SDF). Condition (17) shows how the collateral constraint affects subjective discounting of individuals. When the constraint is not binding, the SDF equals one and intertemporal substitution is based on the world interest rate R_t . The more the constraint binds, the more η exceeds zero, the greater the subjective discounting. Intuitively, the more constrained an agent is today, the more she wants to move resources to today and the less she cares about the future.

Plugging the above into the capital Euler equation (12) shows the impact of the collateral constraint on the portfolio allocation:

$$q_t = \frac{1}{R_t} \mathbb{E}_t \left[(1 - \eta_t)(q_{t+1} + z_{i,t+1} f'(k_{i,t+1}) - \phi_{i,t+1}^1) + \frac{\theta q_{t+1} \eta_{t+1}}{u'(c_t)} \right] - \phi_{i,t}^2 \quad (18)$$

Condition (18) shows that individuals discount expected marginal benefits of capital allocation more the more they are constrained today. As a result, a constrained agent will invest less into re-allocating capital and is stuck with her beginning-of-period industrial specialization.

In combination, the two parts of the financial feedback loop imply that more specialized economies are more likely to become financially constrained in case of adverse productivity

shocks, and financially constrained economies are less able to change their initial specialization. This captures the risk of industrial specialization whereby adverse shocks are both amplified and propagated through this mechanism. This is exacerbates especially shocks with long persistence as a financial constraint suppresses the ability to re-specialize into industries other than the declining one.

3.3 Unregulated Decentralized Competitive Equilibrium

I define and solve for the decentralized equilibrium (DE) in recursive form. I separate individual bond holdings b from the economy's aggregate bond position B on which prices depend. The state variables for the agent's problem are the individual states $\{b, \mathcal{K} = \{k_i\}_{i=\{1,\dots,I\}}\}$, and the aggregate states $\{B, \mathcal{Z} = \{z_i\}_{i=\{1,\dots,I\}}\}$. Aggregate capital is not a state variable because it is in fixed supply. In addition, in order to form expectations of future prices, individuals needs a "perceived" law of motion $B' = \Gamma(B, \mathcal{K}, \mathcal{Z})$ governing the evolution of the economy's bond position, and a conjectured asset pricing function $q(B, \mathcal{K}, \mathcal{Z})$.¹⁶ The individual's recursive optimization problem is:

$$\begin{aligned} V(B, b, \mathcal{K}, \mathcal{Z}) &= \max_{c, b', k'_i} u(c) + \beta \mathbb{E}V(B', b', \mathcal{K}', \mathcal{Z}') \\ \text{s.t. } c + \frac{b'}{R} + q(B, \mathcal{K}, \mathcal{Z}) \sum_i^I k'_i &= \sum_i^I [z_i f(k_i) + q(B, \mathcal{K}, \mathcal{Z}) k_i - \Phi_i(k_i, k'_i)] + b \\ -\frac{b'}{R} &\leq \theta q(B, \mathcal{K}, \mathcal{Z}) \sum_i k_i \\ B' &= \Gamma(B, \mathcal{K}, \mathcal{Z}) \end{aligned} \quad (19)$$

The solution to this problem is characterized by the decision rules $\hat{b}(B, b, \mathcal{K}, \mathcal{Z}), \hat{k}_i(B, b, \mathcal{K}, \mathcal{Z})$, and $\hat{c}(B, b, \mathcal{K}, \mathcal{Z})$. The decision rule for bond holdings induces an "actual" law of motion for aggregate bonds, which is given by $\hat{b}(B, B, 1, \mathcal{Z})$, and the recursive form of (16) induces an asset pricing function $\hat{q}(B, 1, \mathcal{Z})$.

Definition 1 (Recursive Competitive Equilibrium). *A recursive competitive equilibrium is defined by an asset pricing functions $q(B, \mathcal{K}, \mathcal{Z})$, a perceived law of motion for aggregate bond holdings $\Gamma(B, \mathcal{K}, \mathcal{Z})$ and the decision rules $\hat{b}(B, b, \mathcal{K}, \mathcal{Z}), \hat{k}_i(B, b, \mathcal{K}, \mathcal{Z}) \forall i$, and $\hat{c}(B, b, \mathcal{K}, \mathcal{Z})$ with associated value function $V(B, b, \mathcal{K}, \mathcal{Z})$ such that:*

1. *The functions $\{\hat{b}(B, b, \mathcal{K}, \mathcal{Z}), \hat{k}_i(B, b, \mathcal{K}, \mathcal{Z}), \hat{c}(B, b, \mathcal{K}, \mathcal{Z})\}$ and $V(B, b, \mathcal{K}, \mathcal{Z})$ solve the agent's maximization problem, taking as given $q(\cdot)$ and $\Gamma(\cdot)$ as given.*

¹⁶This extends the standard incomplete financial markets model by the term \mathcal{K} (Mendoza, 2010).

2. The market for capital clears: $\sum_i \hat{k}_i(B, b, \mathcal{K}, \mathcal{Z}) = 1$
3. The resource constraint holds: $\hat{c}(B, b, \mathcal{K}, \mathcal{Z}) + \frac{\hat{b}(B, b, \mathcal{K}, \mathcal{Z})}{R} = \sum_i [z_i f(\hat{k}_i(B, b, \mathcal{K}, \mathcal{Z})) - \Phi_i(\hat{k}_i(B, b, \mathcal{K}, \mathcal{Z}), \hat{k}_i(B', b', \mathcal{K}', \mathcal{Z}'))] + B$
4. The perceived and actual laws of motion are consistent: $\Gamma(B, \mathcal{K}, \mathcal{Z}) = \hat{b}(B, B, 1, \mathcal{Z})$ and $\hat{q}(B, \mathcal{K}, \mathcal{Z}) = q(B, \mathcal{K}, \mathcal{Z})$.

3.4 Constrained-efficient Planner Equilibrium

In this section, I consider the optimal policy of a constrained-efficient social planner (SP). The SP chooses allocations internalizing the two key externalities in the economy: the agglomeration externality and the pecuniary externality stemming from the collateral constraint. The SP is subject to the same collateral constraint as the private agents (i.e. he respects that the capital price remains market-determined). In addition to the private agents, however, he understands how the capital price entering the constraint is determined by taking the capital Euler conditions as additional implementability constraints.¹⁷ Let $\{\hat{b}(B, b, \mathcal{K}, \mathcal{Z}), \hat{k}_i(B, b, \mathcal{K}, \mathcal{Z}), \hat{c}(B, b, \mathcal{K}, \mathcal{Z})\}$ be the policy functions that return the values of the corresponding variables in the competitive equilibrium. Taking these functions as given, the SP's optimization problem can be represented in recursive form as follows:

$$\begin{aligned}
V^{SP}(b, \mathcal{K}, \mathcal{Z}) &= \max_{c, b', k'_i, q} u(c) + \beta \mathbb{E} V^{SP}(b', \mathcal{K}', \mathcal{Z}') \quad (20) \\
\text{s.t. } c + \frac{b'}{R} &= \sum_{i=1}^I [z_i f(k'_i) - \Phi_i(k_i, k'_i)] + b \\
-\frac{b'}{R} &\leq \theta q \\
u'(c)(q + \phi_i^2(k_i, k'_i)) &= \beta \mathbb{E}_t \left[u'(\mathcal{C}(b', \mathcal{K}', \mathcal{Z}')) (\mathcal{Q}(b', \mathcal{K}', \mathcal{Z}') + z'_i f'(k'_i) \right. \\
&\quad \left. - \phi_i^1(k'_i, \mathcal{K}_i(b', \mathcal{K}', \mathcal{Z}')) + \theta' \mathcal{Q}(b', \mathcal{K}', \mathcal{Z}') \eta(b', \mathcal{K}', \mathcal{Z}') \right] \forall i \\
\sum_{i=1}^I k_i &= \bar{K} \\
z_i &= \bar{z}_i \cdot k_i^{\xi_i} \quad \forall i
\end{aligned}$$

The economy's resource constraint has a multiplier $\lambda \geq 0$, the collateral constraint $\eta^* \geq 0$ which is different from the private η as private and social values from relaxing the collateral constraint may differ. The implementability constraints for each industry i have multipliers $\delta_i \geq 0$, and the market clearing Lagrange multiplier is denoted by Ξ .

¹⁷This extends the model by Mendoza (2010) to a multi-industry setting.

Definition 2 (Recursive Constrained-efficient Equilibrium). *The recursive constrained-efficient equilibrium is defined by the policy functions $k_i(b, \mathcal{KZ})$, and $b(b, \mathcal{KZ})$ with associated decision rules $\hat{c}(b, \mathcal{K}, \mathcal{Z})$, $\eta^*(b, \mathcal{K}, \mathcal{Z})$, the pricing function $q(b, \mathcal{K}, \mathcal{Z})$ and value function $V(b, \mathcal{K}, \mathcal{Z})$, and the associated decision rules $\mathcal{C}(b, \mathcal{K}, \mathcal{Z})$, $\eta(b, \mathcal{K}, \mathcal{Z})$ and asset prices $\mathcal{Q}(b, \mathcal{K}, \mathcal{Z})$ such that the following conditions hold:*

1. *Planner's optimization: $V(b, \mathcal{K}, \mathcal{Z})$ and the functions $b(b, \mathcal{KZ})$, $k_i(b, \mathcal{KZ})$, $\hat{c}(b, \mathcal{K}, \mathcal{Z})$, $\eta^*(b, \mathcal{K}, \mathcal{Z})$ and $q(b, \mathcal{K}, \mathcal{Z})$ solve the Bellman equation defined in Problem (20) given $\mathcal{C}(b, \mathcal{K}, \mathcal{Z})$, $\eta(b, \mathcal{K}, \mathcal{Z})$ and $\mathcal{Q}(b, \mathcal{K}, \mathcal{Z})$.*

Efficiency and optimal policy. Efficiency in this economy can be characterized by the difference between the planner and private agents' solutions. This difference can be summarized by two key components. On the one hand, the existence of the agglomeration externality which private agents fail to internalize. On the other hand, the effect of current capital allocation (i.e. portfolio allocation) and bond holdings (i.e. consumption vs saving) on the likelihood of becoming financially constraint via the price of capital and the existence of the collateral constraint. I refer to the latter as the pecuniary externality.

I characterize these differences by defining the following planner optimality conditions:

$$c_t :: \lambda_t = u'(c_t) - \frac{u''(c_t)}{u'(c_t)} \theta_t \eta_t^* q_t - u''(c_t) \sum_{i=1}^I \delta_{i,t} \phi_{i,t}^2 \quad (21)$$

$$q_t :: \sum_{i=1}^I \delta_{i,t} = \frac{\theta_t \eta_t^*}{u'(c_t)} \quad (22)$$

$$k_{i,t+1} :: \lambda_t \phi_{i,t}^2 = \beta \mathbb{E}_t \left[\lambda_{t+1} (\bar{z}_{i,t+1} (\xi_i + \alpha) k_{i,t+1}^{\xi_i + \alpha - 1} - \phi_{i,t+1}^1) + \sum_{i=1}^I \delta_{i,t} \Omega_{i,t+1}^K \right] + \Xi \quad (23)$$

$$b_{t+1} :: \lambda_t = \beta R_t \mathbb{E}_t \left[\lambda_{t+1} + \sum_{i=1}^I \delta_{i,t} \Omega_{i,t+1}^B \right] + \eta_t^* \quad (24)$$

where Ω^B and Ω^K collect all terms with derivatives that capture the effects of the SP's choice of b' and k'_i via all implementability constraints. They are further discussed in Appendix (B.1). The socially optimal policy can be defined in terms of the social *value of wealth, portfolio allocation and consumption vs savings* choice.

Condition (21) presents the social *value of wealth*. It extends the private value, which takes the standard form $\lambda_t = u'(c_t)$, by two terms. The second term on the right-hand side corresponds to the amount by which an additional unit of consumption reduces marginal utility and relaxes the collateral constraint by raising the asset price. This term is standard in recent incomplete market models (Bianchi and Mendoza, 2018). Note, that the term disappears when the collateral constraint is currently non-binding, and $\eta_t^* = 0$. The third

term on the right-hand side reflects the amount by which an additional unit of consumption reduces marginal utility and relaxes each industry's implementability constraint at the adjustment costs ϕ_i . The relaxation of each implementability constraint depends on how strongly each constraint binds which is summarized by the shadow price δ_i . Condition (22) shows that given that the capital market clears, the combination of industry shadow prices equals zero as long as the constraint binds. As soon as the constraint binds, shadow prices do not perfectly offset each other.

Condition (23) presents the socially optimal *portfolio allocation*. It deviates from the private agents' allocation in two ways. First, the planner internalizes industry-specific agglomeration economies. Consequently, the social marginal product of capital in industry i exceeds the private marginal product by the term ξ_i . Second, the planner internalizes the pecuniary externality: the effect of capital allocation on the equilibrium price of capital. This is captured by the term $\sum_{i=1}^I \delta_{i,t} \Omega_{i,t+1}^K$. Intuitively, the planner understands that shifting capital between industries alters its price, which in turn affects the tightness of future borrowing constraints. The shadow value of these constraints is captured by the Lagrangian multipliers embedded in $\Omega_{i,t+1}^K$. This mechanism introduces a portfolio allocation channel for financial amplification, extending the framework of Bianchi and Mendoza (2018) to a multi-industry economy. As a result, the economy's degree of specialization (not just its aggregate bond holdings or marginal utility of consumption) becomes a determinant of its vulnerability to financial shocks.

Condition (24) governs the social planner's optimal consumption-savings decision. Unlike private agents, the planner internalizes the pecuniary externality that aggregate debt imposes on the price of capital. This effect, captured by the term $\sum_{i=1}^I \delta_{i,t} \Omega_{i,t+1}^B$, reflects how an additional unit of debt today tightens future borrowing constraints. Intuitively, higher debt reduces the economy's flexibility to adjust its capital structure and moves it closer to the collateral limit, thereby increasing the likelihood of a binding constraint. This mechanism extends the one identified in Bianchi (2011) by incorporating the additional channel of capital allocation. Furthermore, the planner's valuation of the collateral constraint, represented by the Lagrangian multiplier η^* , differs from the private multiplier because the social value of relaxing the constraint is not fully internalized by individual agents.

I now show that the planner's equilibrium can be decentralized with a state-contingent tax on debt τ_t^B and on industry-specific marginal product of capital τ_t^K . The price of bonds becomes $\frac{1}{R(1+\tau_t^B)}$ in the budget constraint of the private agent in the regulated competitive equilibrium. The marginal return on capital becomes $(1 + \tau_{i,t}^K) z_{i,t} k_{i,t}^{\alpha+\xi_i-1}$. The tax revenue rebated using a lump-sum transfer T_t . The agent's Euler conditions for bonds and capital

become:

$$u'(c_t)(q_t + \phi_{i,t}^2) = \beta \mathbb{E}_t [u'(c_{t+1})(q_{t+1} + (1 + \tau_{i,t+1}^K)z_{i,t+1}f'(k_{i,t+1}) - \phi_{i,t+1}^1) \\ + \theta_{t+1}q_{t+1}\eta_{t+1}] \quad (25)$$

$$u'(c_t) = \beta R_t(1 + \tau_t^B) \mathbb{E}_t[u'(c_{t+1})] + \eta_t. \quad (26)$$

Proposition 1 (Decentralization with taxes and subsidies). *The constrained-efficient equilibrium can be decentralized with a state-contingent tax on debt, and an industry-specific tax (subsidy) with tax revenue rebated as a lump-sum transfer and the tax rates set to satisfy:*

$$1 + \tau_t^B = \frac{1}{\mathbb{E}_t[u'(t+1)]} \left[\sum_i \delta_{i,t} \Omega_{i,t+1}^B - \frac{u''(t+1)}{u'(t+1)} \theta \eta_{t+1} q_{t+1} - u''(t+1) \sum_i \delta_{i,t+1} \phi_{i,t+1}^2 \right] \\ + \frac{1}{\beta R_t \mathbb{E}_t[u'(t+1)]} \mathbb{E}_t \left[\frac{u''(t)}{u'(t)} \theta \eta_t q_t + u''(t) \sum_i \delta_{i,t} \phi_{i,t}^2 \right] \quad (27)$$

$$1 + \tau_{i,t}^K = \frac{1}{\mathbb{E}_t[\alpha z_{i,t+1} k_{i,t+1}^{\alpha+\xi_i-1}]} \left[\left(u'(t+1) - \frac{u''(t+1)}{u'(t+1)} \theta \eta_{t+1} q_{t+1} - u''(t+1) \sum_i \delta_{i,t+1} \phi_{i,t+1} \right) \right. \\ \left. ((\alpha + \xi_i) z_{i,t+1} k_{i,t+1}^{\alpha+\xi_i-1} - \phi_{i,t+1}^1) + \sum_i \delta_{i,t} \Omega_{i,t+1}^K \right. \\ \left. - u'(t)(q_{t+1} - \phi_{i,t}^1) - \theta \eta_{t+1} q_{t+1} \right] \\ + \frac{1}{\beta \mathbb{E}_t[\alpha z_{i,t+1} k_{i,t+1}^{\alpha+\xi_i-1}]} \left(u'(t) q_t + \Xi + \phi_{i,t}^2 u''(t) \sum_i \delta_{i,t} \phi_{i,t}^2 \right) \quad (28)$$

where the arguments of the functions have been shorthanded as dates to keep the expression simple. The proof can be found in Appendix (B.2).

There are three sources of inefficiencies the planner aims at alleviating with the two optimal tax schedules on debt and capital allocation. On the one hand, the planner addresses the pecuniary externality stemming from debt. Private agents fail to internalize the effect of their aggregate bond holdings on the future price of capital, q_{t+1} , and thus on the tightness of future collateral constraints. The state-contingent tax on debt, τ_t^B , corrects this overborrowing externality. By comparing the agent's Euler equation for bonds (26) with the planner's condition (24), it becomes evident that τ_t^B is set to precisely offset the wedge between the private and social valuation of debt, forcing agents to internalize the social costs captured by the $\sum_{i=1}^I \delta_{i,t} \Omega_{i,t+1}^B$ term.

On the other hand, two distinct inefficiencies plague the allocation of capital. First, a technological externality arises as agents do not account for industry-specific agglomeration economies, ξ_i . Second, another pecuniary externality exists because agents overlook how their portfolio choices today affect future asset prices through the $\sum_{i=1}^I \delta_{i,t} \Omega_{i,t+1}^K$ term.

The industry-specific tax on capital, $\tau_{i,t}^K$, is an instrument that corrects both distortions simultaneously. Note, that the nature of this instrument is state- and industry-specific. Hence, the optimal policy will generally involve subsidies for some industries and taxes for others. It adjusts the private marginal return on capital to reflect its true social marginal product, which incorporates both the agglomeration benefits and the general equilibrium effects on financial constraints. By appropriately setting this tax schedule, the planner aligns the private portfolio condition (25) with the social optimum (23). In this way, the combination of these two policy instruments decentralizes the planner's allocation, restoring efficiency by compelling private agents to confront the full social consequences of their financial decisions.

4 Quantitative analysis

In this section, I study the model's implications by conducting simulations for a baseline calibration. I then use the model to perform four exercises, which together quantify the contribution of industrial specialization to growth. First, I show the impulse responses in capital portfolio allocation and bond holdings to reductions in a single industry's productivity, incorporating the endogenous responses arising from the financial amplification. This provides the answer on how specialization affects growth in the model. Second, I simulate economies with different initial levels of industrial specialization replicating the specialization trade-off documented empirically, and highlighting the relevance of the financial amplifier. Third, I assess the welfare implications of feasible industries-specific subsidies and taxes, and taxes on debt.

4.1 Calibration

I calibrate the model using regional US Census and BEA data between 1950 and 2020 at a decadal frequency.¹⁸ Due to data availability I will predominantly focus on industries within manufacturing for the years before 1987 and use less frequent data for more industries only in a descriptive sense. After 1987, I supplement the manufacturing data with data on all industries. For some variables, I will use only U.S. data because of data limitations. The functional forms for preferences and adjustment costs are the following:

$$u(c_t) = \frac{c_t^{(1-\gamma)} - 1}{(1 - \gamma)} \quad \gamma \geq 0$$

¹⁸As an extension, I also provide results at the annual level as shown appendix (??).

$$\Phi_i(k_{i,t}, k_{i,t+1}) = \frac{\Phi_i}{2} \left(\frac{k_{i,t+1}}{k_{i,t}} - 1 \right)^2 k_{i,t} \quad \Phi_i \geq 0 \quad \forall i$$

with coefficient of risk aversion γ and the adjustment cost parameter Φ_i .

The calibration proceeds in two steps. First, a subset of parameter values are set using direct empirical evidence or standard values from the literature. Second, given these parameter values, the remaining parameters are determined by solving the model to jointly target moments from the data.

In the first step, I set the parameters of the productivity processes and the values of $\{\gamma, \alpha, \{\Phi_i, \xi_i\}_{i=\{1, \dots, I\}}, \theta\}$, the parameters of the the R process and the industry-specific TFP processes. The relative risk aversion (or inverse inter-temporal elasticity of substitution) γ is an important parameter because it affects the magnitudes of price adjustments as well as the curvature of the stochastic discount factor when the collateral constraint binds. For a given η , an increase in γ will raise stochastic discounting and thereby reduce the portfolio allocations of individuals. In choosing the risk aversion parameter, I aim to accommodate the estimates of two relevant strands of literature. On the one hand, the real business cycle literature uses a risk aversion of around $\gamma = 2$ (Mendoza, 2010). On the other hand, the finance and asset pricing literature estimates risk aversion between 7.5 and 10 (Bansal, Kiku, and Yaron, 2016). In order to accommodate both literature I choose a baseline risk aversion of $\gamma = 5$ and perform robustness exercises for the boundary values. The income share of capital α is set to be 0.3 reflecting the average historical U.S. capital income share in line with vast existing literature.

The values for industry-specific convex capital adjustment costs are taken jointly from Hall (2004) and Groth and Khan (2010). The former paper estimates adjustment costs from capital Euler equations using US firm-level data over the period 1948 through 2001, and the latter provides updated estimates until 2010. Estimates are reported at the 2-digit SIC industry level of manufactured goods. The detailed table of Φ_i is shown in Appendix (A.6). The calibration of this parameter reveals two important aspects. First, industries vary significantly in their capital specificity and are subject to largely different adjustment costs (e.g. fabricated metal industries have more than 50% larger adjustment costs than wood products). It is therefore important to account for these differences in the multi-industry setting of the model. Second, a more than one third of all industries have adjustment costs that are close to (or statistically indifferent from) zero at the annual level. In these industries real factor adjustment costs can therefore only play a minor role in generating persistence of capital allocation.

The values for industry-specific agglomeration strengths are taken directly from the estimates reported by Bartelme et al. (2019) and are shown in Appendix (A.6). The authors

estimate sector-level scale elasticities using predicted demand as instruments based on trade shares, population and sector size at the 2-digit SIC level. Data limitation allows them to base their estimates only on the year since 1995. In this paper, I therefore assume that agglomeration externalities have remained constant over time. I further assume agglomeration economies to be constant across space such that a single industry generates the same agglomeration irrespective of whether it is located in, for example, Dayton, Ohio or Rochester, Minnesota.

The credit regime value θ is set to be consistent with the average US aggregate corporate leverage over time reported by Graham, Leary, and Roberts (2015). The authors construct a century-long panel of US firm data showing that the loan-to-value (LTV) ratio of firms has fluctuated relatively little in the $\theta = [0.3, 0.4]$ range. Their estimates coincide with other studies in the financial amplification literature targeting the frequency of crisis (see, e.g. Bianchi (2011) and Gertler and Karadi (2011)). In the baseline calibration, I assume this value to be constant over time. Importantly, the authors define both market and book value estimates where only the former are relevant in the context of this paper.

The industry-specific TFP follows independent, trend-stationary AR(1) processes given by equation (7). The shocks $\epsilon_{i,t}$ are discretized using Tauchen's quadrature method with 15 realizations for each shock. I use the 2-digit manufacturing industry-specific TFP measure following Becker, Gray, and Marvakov (2021) for the 1958 - 2018 period, the longest time series available from official sources. In order to estimate the processes, I follow a two-step procedure. First, I normalize all TFP by the weighted-averaged TFP across all industries. Then, I estimate relative HP-filtered cyclical and trend components for each industry as given in Appendix (A.6).

The gross interest rate follows an independent AR(1) process.¹⁹ In line with standard approach in the international macro literature Bianchi and Mendoza (2018), I calibrate the interest-rate process by measuring the annualized ex-post return on 90-day U.S. T-bills from the official FRED source. This yields $\bar{R} = 1.013$ with persistence $\rho_R = 0.01$ and variance $\sigma_R = 0.0186$.

The second stage of the calibration is to jointly set the values of $\{\{k_{i,1950}\}_{i \in \{1, \dots, I\}}, \beta\}$. I invert the model given the externally calibrated capital share α , the agglomeration ξ_i and the 1950 industry TFP $z_{i,1950}$ in order to back out the initial capital stocks (i.e. the initial specialization) for every commuting zone. The target for setting the value of β is an estimate of the average net foreign asset position (NFA) as a share of GDP at 1976 - the earliest available official NFA estimate. In line with existing literature, I do not target the time series average because the U.S. NFA-GDP ratio has displayed a marked

¹⁹This assumption is in line with the observation that the Basu-Fernald U.S. Solow residual estimates are uncorrelated with the U.S. real interest rate on 90-day Tbills.

downward trend since the early 1980s due to the Global Imbalances phenomenon (Bianchi and Mendoza, 2018). The model’s decentralized equilibrium yields an unconditional mean of b as a share of GDP that matches the NFA-GDP ratio with $\beta = 0.95$.

Parameter	Value	Source or Target
<i>Parameters set externally</i>		
Risk Aversion	$\gamma = 5$	Average value in literature
Capital Share	$\alpha = 0.3$	Avg. US capital income share
Adjustment Costs	$\Phi_i \in [0, 3.26]$	Hall (2004); Groth (2010)
Agglomeration	$\xi_i \in [0.1, 0.29]$	Bartelme et al. (2024)
Collateral regime	$\theta = 0.35$	Historical LTV ratio (Graham et al, 2015)
Interest Rate	$\bar{R} = 1.3\%, \rho_R = 0.01$ $\sigma_R = 0.0186$	U.S. 90-day T-Bills
TFP Process	$\rho_i \in [0.71, 0.9]$ $\sigma_i \in [0.013, 0.027]$	Std. and autoc. of U.S. industry TFP
<i>Parameters set internally</i>		
1950 capital stock	$k_{i,1950} \in [0.1, 0.29]$	Matching income shares
Discount Factor	$\beta = 0.95$	Avrg. NFA position = -20% of GDP

Table 2: Model Calibration

The model is solved using a global, nonlinear solution algorithm taking into account the occasionally binding, stochastic collateral constraint. The DE solution is obtained using a time iteration algorithm. Following Bianchi (2011), in the SP’s problem, I use a nested fixed-point algorithm: The inner loop solves for policy functions and the out one updates future policies given the solution to the Bellman equation. The existence of multiple, independent productivity processes requires an additional state variable capturing the state of relative productivities at every point in time. Appendix (B.3) describes the algorithm in further detail.

4.2 The specialization trade-off

I first apply the calibrated model to understand U.S. regional growth since 1950. To investigate the mechanisms through which specialization determines income and long-run growth, I conduct a simulation of the universe of U.S. commuting zones, treating each as an individual small open economy. The simulation spans a 70-year period, initialized using the observed 1950 specialization patterns and driven by the realized productivity processes observed across industries. For the purposes of this exercise, I make several simplifying assumptions.

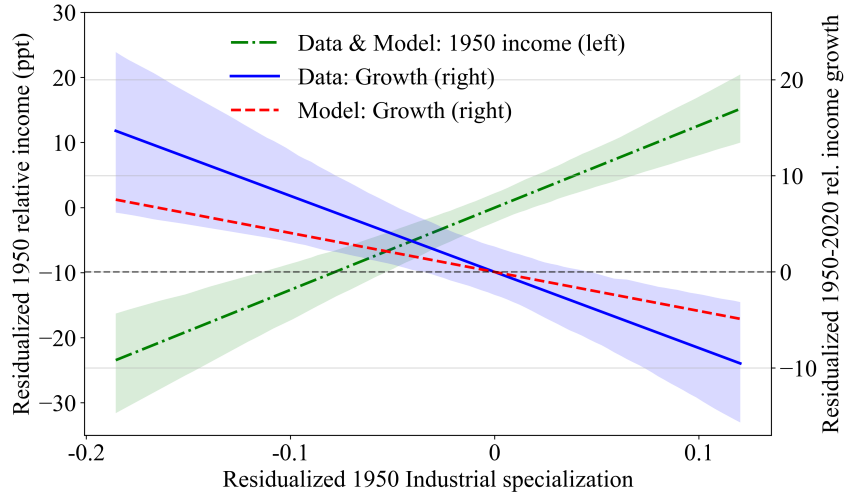


Figure 5: The specialization trade-off: Data vs Model

Notes: Figure (5) compares the model's simulated effect of specialization on long-run growth (red dotted line) with the observed empirical data. The 70-year simulation is initialized to exactly match the specialization patterns and income levels of U.S. commuting zones in 1950.

First, the industrial landscape is condensed into two sectors: industrial machinery and a composite rest of manufacturing. By focusing on specialization within the manufacturing sector, this approach abstracts from broader structural change issues between manufacturing and other parts of the economy. This is a reasonable simplification, as the main empirical section explicitly controls for structural change using a shift-share instrument. Second, the rest of manufacturing sector serves as a proxy for a diversified industrial base, representing a safe portfolio of industries. Specialization is hence the concentration of capital across the two sectors. Finally, the simulation is calibrated to directly match the initial specialization shares and resulting income levels for every commuting zone in 1950, ensuring the model's starting conditions match the historical data exactly.

I compare the growth across the economies as a result of the initial specialization and the endogenous re-specialization in response to productivity changes. Figure (5) shows that the model can explain roughly half of the long-run growth decline implied by 1950 specialization. The figure further rationalizes the two key aspects of the specialization trade-off. First, greater specialization implies higher short-run income. In the model this is the result of both industry-specific agglomeration and initial capital allocation across industries. The model matches this exactly by default as given industry-specific productivity, agglomeration strength and capital income shares, the initial capital allocations is calibrated to match the observed per capita income differences.

Second, greater initial specialization results in lower long-run growth. This is the result of two mechanisms. On the one hand, the difference in long-run productivity growth

across industries in combination of the distribution of initial specialization and the capital adjustment costs creates a mechanical difference in growth rates. On the other hand, the endogenous amplification of the industry-specific shocks through the collateral constraint generates an additional response based on initial industrial specialization.

Figure (6) decomposes the effect of specialization on long-run growth by the two frictions. The financial friction generates 56% of the effect of specialization on growth. In absence of the financial frictions, the convex adjustment costs alone capture less than one fourth of the heterogeneity in growth based on specialization. This result highlights the crucial role of financial amplification in explaining long-run growth outcomes, a channel whose quantitative importance this paper underscores. In contrast, the minor effect of adjustment costs aligns with the findings in existing literature (e.g., Hall (2004)) that point towards small empirically estimated adjustment costs across industries.

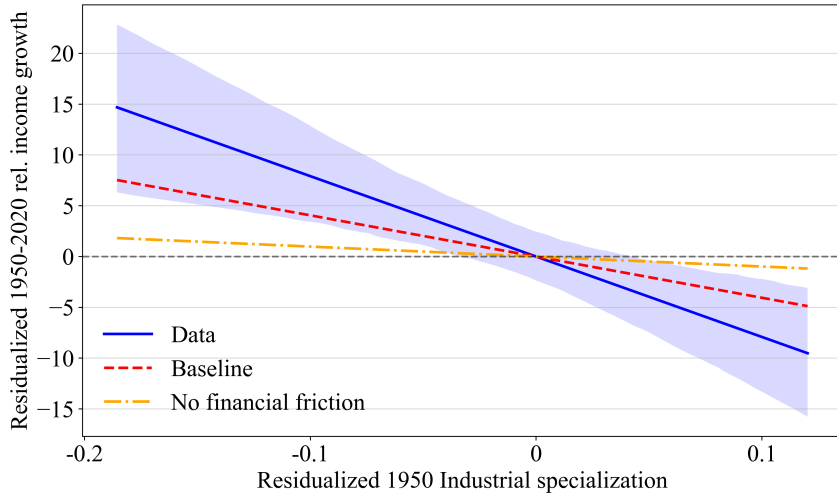


Figure 6: The role of financial amplification for growth

Notes: Figure (6) decomposes the effect of specialization on 70-year income growth. It compares the relationship observed in the data with two simulations: the baseline model (which includes both financial frictions and adjustment costs) and a counterfactual model without financial frictions.

4.3 Specialization dynamics

In order to analyze the dynamics of regional specialization, I now consider the impulse response to an adverse, one standard deviation transitory shock to a single industry. Figure (7) shows the responses of bond holdings, capital allocation to the shocked industry, consumption and the capital price for an economy with and without the collateral constraint beginning from a stationary equilibrium. Two central messages arise from this exercise.

First, the dynamics of the shock are hump-shaped and propagated. In response to the

decline of productivity, agents experience a reduction in income. They borrow in order to allocate capital away from the shocked industry and in order to smooth consumption over time. The price of the capital falls as future discounted dividends decline with the marginal product of capital.

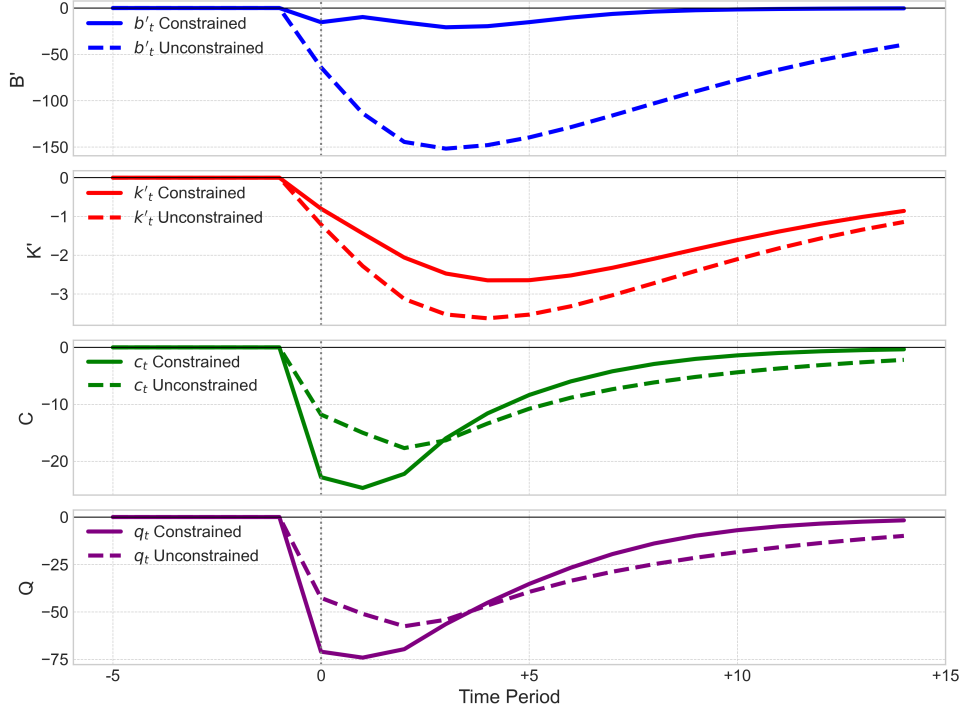


Figure 7: Impulse Responses to a transitory industry-specific productivity shock

Notes: Figure (7) shows the impulse response functions to a one-standard-deviation adverse productivity shock in a single industry. It compares the response in the baseline model to a counterfactual model without financial frictions.

Second, comparing the constrained and the unconstrained economy highlights the relevance of the collateral constraint in amplifying and propagating the shock. While the unconstrained economy has unlimited borrowing capacity, the constrained economy faces a financial amplification that affects both capital allocation and consumption smoothing ability. IN response to the shock, borrowing agents hit the constrained/ This has two immediate effects. First, the standard financial amplifier effect: in order to consume more today, agents start fire-selling capital which reduces the price of capital further and further tightens the borrowing constraint. The amplifier results in the difference between the unconstrained and constrained economies in the bond holdings, consumption and capital price responses. Second, the capital allocation amplifier: constrained agents are less able to invest in capital and pay the re-allocation costs. With greater stochastic discounting they care less about the marginal benefits of re-allocating capital for tomorrow and show a much more sluggish response in capital allocation. The collateral constraint thus implies that agents are stuck with their initial specialization and do invest as much to benefit from

capital in more productive industries. This is the key novel driver of persistent industrial specialization.

4.4 Capital allocation, borrowing decisions and amplification

In this section, I solve for the competitive bond and capital accumulation decisions. Figure 8a shows the bond policy for a productivity shock to one industry for an economy that is relatively specialized in that industry (e.g. Dayton, Ohio) vis-à-vis an economy that has a diversified portfolio of capital across industries (e.g. Rochester, Minnesota). The graph reveals two key mechanisms. First, without the endogenous borrowing constraint, the policy function for next period's bond holdings would be monotonically increasing in current bond holdings. In line with the standard financial amplification mechanism (Bianchi, 2011), the policy functions are nonmonotonic. The change in the sign of the slope indicates the point at which the credit constraint binds. To the right of this point, the credit constraint is slack and bond decision rules display the usual upwards-sloping shape. To the left of this point, the financial amplifier is at play, where a fall in the price of capital tightens the constraint forcing a fire-sale of capital which further reduces the price and further tightens the borrowing constraint.

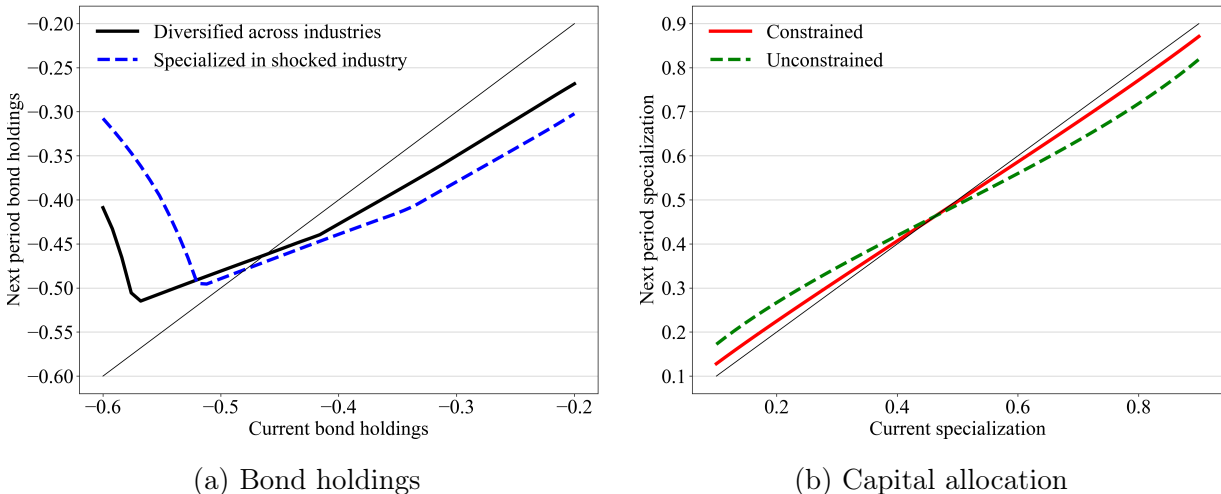


Figure 8: Policy functions for a negative one-standard deviation industry-specific shock

Notes: Figure 8 shows the decision rules for bond holdings and capital allocation following a one-standard-deviation adverse productivity shock to a single industry.

The second mechanism is evident when comparing the two lines and highlights the role of specialization for borrowing decisions and captures the key novel features. The economy specialized in the shocked industry will be more exposed to the same shock and therefore try to borrow more for any current bond position. Given the stronger fall in the capital price, this economy will hit the borrowing constraint for a higher initial bond position.

Intuitively, the more specialized a economy, the more likely it is to become borrowing constraint in response to a shock to that industry. This mechanism extends the standard financial amplification mechanism to a multi-industry setting.

Figure 8b shows the capital allocation decision rules: the current share of capital allocated to the industry shocks is given by the horizontal axis, and tomorrow's share of capital in the same industry on the vertical axis. The decision rules are plotted for economies: one that is borrowing constraint and one that is unconstrained. Again, the graph can be interpreted in two steps. First, observe that the slope of the decision rules is smaller than 45 degrees. Hence, in response to an adverse shock to one industry, agents re-allocate capital away from that industry towards the rest of the economy. Second, the ability to re-allocate capital towards other industries is directly affected by the tightness of the borrowing constraint. A constrained economy will be less able to buy new capital and pay the re-allocation costs than an unconstrained economy. This is a combination of the lower liquidity of constraint agents as well as the greater stochastic discounting of any future benefits of capital allocation shown in (18).

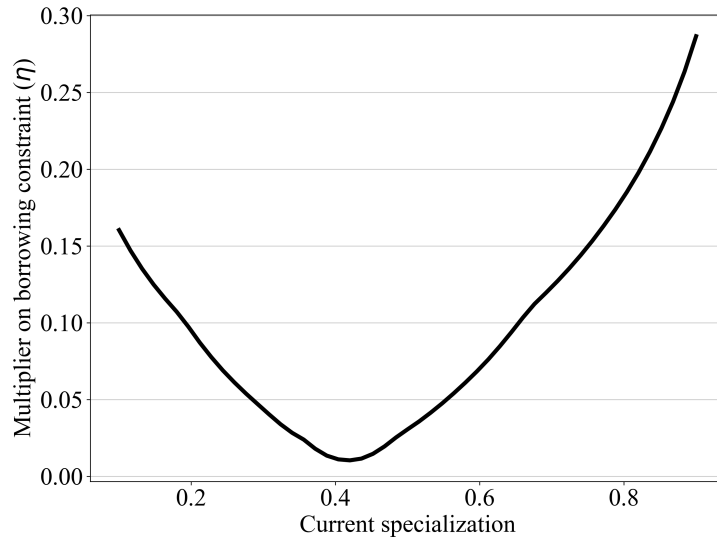


Figure 9: Specialization and the tightness of the collateral constraint

Notes: Figure (9) Lagrangian multiplier on the collateral constraint over current bond holdings for an adverse one standard deviation productivity shock to a single industry.

The role of current specialization for the likelihood of becoming borrowing constraint is summarized in Figure (9). The figure shows the Lagrangian multiplier on the collateral constraint as a function of current capital allocation in the shocked industry. The resulting line depicts a U-shaped curve. The low-point of the curve corresponds to a diversified economy in which capital is evenly allocated across the two industries (i.e. Machinery and the rest of manufacturing). To the right of this point, the tightness of the collateral constrain increases with the degree of specialized in the shocked industry. The fact that

the tightness also increases to the left of this points reflects the forward-looking behavior of agents and the capital price. Intuitively, agents that are relatively specialized in the non-shocked industry understand that given their expectation of industry-specific shocks they are over-specialized in the other industry. This understanding is incorporated in the discounting for future expected dividends and leads to a reduction in the capital price today already which tightens the borrowing constraint.

The combination of the bond and capital allocation decision rules capture the novel propagation and financial amplification mechanism of industrial specialization in this model. The feedback loop consists of two parts. On the one hand, greater industrial specialization increases exposure to industry-specific shocks and thereby raises the likelihood of becoming borrowing constraint. On the other hand, borrowing constraint agents are less able to invest into new capital and change their current portfolio of capital across industries. This generates persistence of specialization for highly specialized regions that are hit by an adverse shock to their main industry by suppressing investment. At the same time it generates amplification to negative shocks and introduces an asymmetry in the response to productivity fluctuations.

5 Constrained-efficient allocation and welfare

In this section, I address the normative question of this paper: What is the optimal degree of regional specialization? I compute the optimal capital allocation and borrowing decision implemented by a constrained-efficient planner that I have in section (3). I then proceed in two steps. First, I show how and why the planner equilibrium differs from the competitive one. Then, I present the welfare difference across the two equilibria.

Two sources of inefficiency motivate the planner to deviate from the competitive equilibrium. First, a positive agglomeration externality incentivizes more specialization. The planner internalizes that the social return to concentrating capital exceeds the private return, as individual agents fail to account for how their investments collectively boost industry-level productivity. This motivates the planner to favor a higher degree of industrial concentration than arises in the decentralized equilibrium.

Second, a pecuniary externality, stemming from financial frictions, creates a countervailing incentive for diversification. Individual agents do not internalize how specializing makes the aggregate value of collateral more volatile and exposed to sectoral shocks. The planner recognizes this heightened volatility increases the probability of future borrowing constraints becoming binding across the economy. Consequently, the planner favors diversification as a form of insurance to mitigate this systemic financial risk.

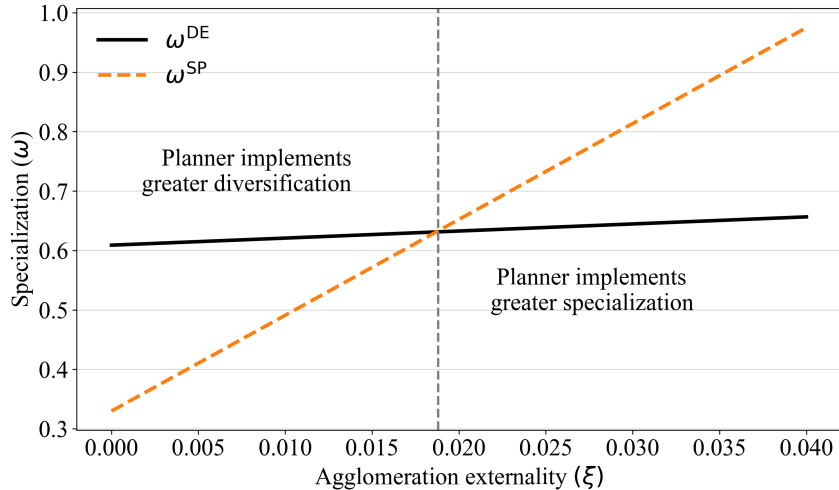


Figure 10: Competitive vs constrained-efficient specialization trade-off

Notes: Figure (9) compares the socially optimal level of specialization with the competitive equilibrium outcome, plotted against the strength of agglomeration forces in a single industry.

Figure (5) summarizes the difference between the socially optimal and private specialization trade-off. I show the regional specialization relative to the strength of agglomeration calibrated using the 1950 level of industry productivities. The graph reveals three key aspects. First, in absence of agglomeration, the competitive equilibrium is over-specialized in too few industries. Private agents fail to internalize the financial amplification to sectoral shocks stemming from the pecuniary externality, and expose the economy too much to becoming borrowing constraint. Instead, the planner will diversify the economy to limit the likelihood of hitting the collateral constraint in response to adverse shocks.

Second, as agglomeration forces strengthen, specialization increases in both equilibria, but more steeply in the planner's allocation. While private agents respond only to the private productivity gains, the planner also internalizes the positive social returns from agglomeration, creating a stronger incentive to concentrate capital. This leads to a unique crossover point where the two opposing inefficiencies—the negative financial externality and the positive agglomeration externality—perfectly offset each other. At this point, the competitive equilibrium is coincidentally socially optimal.

Third, beyond the crossover point, the agglomeration externality dominates the financial risk. The social benefits of concentrating production now outweigh the costs of financial fragility. Consequently, the planner's equilibrium becomes more specialized than the competitive equilibrium. This outcome aligns with the vast literature in economic geography and trade where specialization is typically found to be welfare-improving (see, e.g. Bartelme et al. (2019)).

Welfare. In line with Bianchi (2011), I compute welfare gains from correct the two opposing externalities as the proportional increase in consumption for all possible future histories in the decentralized equilibrium that would make private agents indifferent between remaining in the decentralized equilibrium and correcting the externalities. Because of the homotheticity of the utility function, the welfare gains Λ at a state $(b, \sum_i k_i)$ is given by:

$$(1 + \Lambda(b, \sum_i k_i)^{(1-\gamma)}) V^{DE}(B, b, \sum_i k_i) = V^{SP}(b, \sum_i k_i) \quad (29)$$

Figure (11) quantifies the welfare gains from the planner's optimal policy following a one-standard-deviation adverse productivity shock. The gains are evaluated across the economy's initial state, defined by its asset position and degree of specialization. Panel (11a) shows that welfare gains are greatest for the most indebted economies. Intuitively, regions with large negative bond holdings are more financially fragile and operate closer to their borrowing limit. The planner's policy provides insurance by encouraging higher savings (i.e., holding more bonds) and reallocating capital to reduce the probability of the borrowing constraint binding after a shock. This intervention is most valuable for economies initially on the brink of financial distress.

Panel (11b) reveals a U-shaped relationship between the welfare gains and the initial level of specialization. Gains are substantial in both tails. For highly specialized regions, the planner corrects the competitive equilibrium's failure to account for systemic financial risk. For highly diversified regions, the planner pushes for more concentration to reap the benefits of agglomeration externalities that private agents ignore. The gains are minimized for regions where the initial level of specialization happens to be near the optimal trade-off between agglomeration benefits and financial risk, the point where the two externalities largely offset each other, as illustrated previously in Figure (10).

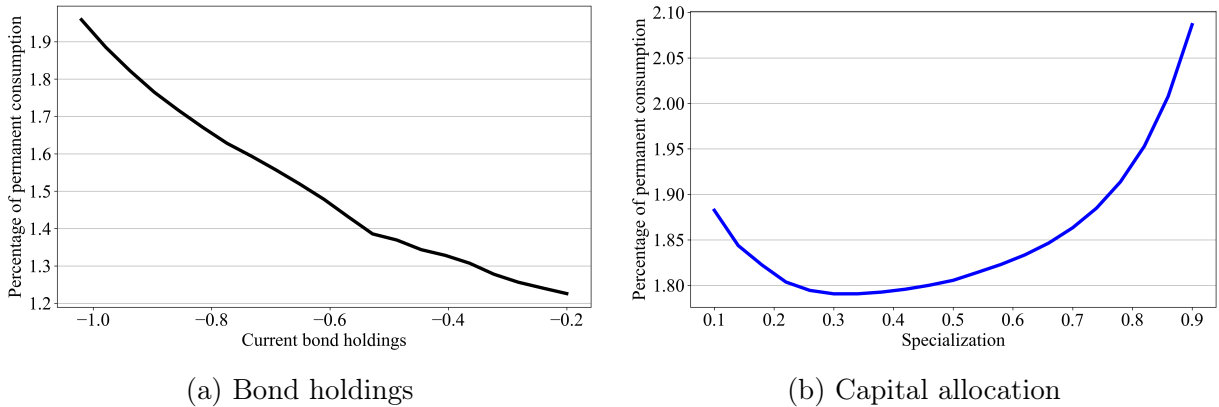


Figure 11: Welfare gains for a negative one-standard deviation industry-specific shock

Notes: Figure (11) shows the welfare gain of the constrained-efficient planner allocation over current bond holdings and specialization.

6 Conclusion

In this paper, I show that industrial specialization of regions is crucial for understanding regional income and growth differences. For my analysis, I use regional growth differentials across 722 US commuting zones since 1950. I document three novel facts. First, commuting with high industrial specialization in 1950 have higher per capita income initially but experience persistently lower growth in the long-run. This highlights a specialization trade-off where regions benefit from focusing resources on a specific industry today but may be persistently worse off if this industry declines. Second, as regions grow, they become more specialized (and vice versa). Third, the specialization at the region-industry level, however, is highly persistent.

Given this empirical evidence, I develop a dynamic multi-region, multi-sector model to link specialization to growth and formalize the trade-off between benefits and costs of specialization. The model's key innovation is to endogenize the costs of specialization by showing how it can lead to persistently lower long-run growth. The costs arise through adjustment costs and a financial friction. The quantitative model, disciplined by U.S. Census data on commuting zones, reveals that more than half of the adverse effect of specialization on growth can be attributed to the financial friction. A constrained efficient planner allocation that internalizes the benefits of specialization through agglomeration externalities, and the costs of specialization through the financial frictions highlights the potential for industrial policy. By balancing the two opposing force when allocating factors, the planner increases welfare by 1.2 to 2.2 percent depending on the region. This paper offers the potential vast future research, including cross-regional spillovers of specialization and aggregate growth implications of regional specialization.

References

- Allen, Treb and Costas Arkolakis (2014). “Trade and the Topography of the Spatial Economy”. In: *The Quarterly Journal of Economics* 129.3, pp. 1085–1140.
- Autor, David, David Dorn, et al. (2020). “The fall of the labor share and the rise of superstar firms”. In: *The Quarterly Journal of Economics* 135.2, pp. 645–709.
- Autor, David, Lawrence F Katz, and Melissa S Kearney (2008). “Trends in US wage inequality: Revising the revisionists”. In: *The Review of economics and statistics* 90.2, pp. 300–323.
- Autor, David, Christina Patterson, and John Van Reenen (2023). *Local and national concentration trends in jobs and sales: The role of structural transformation*. Tech. rep. National Bureau of Economic Research.
- Bansal, Ravi, Dana Kiku, and Amir Yaron (2016). “Risks for the long run: Estimation with time aggregation”. In: *Journal of Monetary Economics* 82, pp. 52–69.
- Barro, Robert J and Xavier Sala-i-Martin (1992). “Convergence”. In: *Journal of political Economy* 100.2, pp. 223–251.
- Bartelme, Dominick G et al. (2019). *The textbook case for industrial policy: Theory meets data*. Tech. rep. National Bureau of Economic Research.
- Becker, Randy, Wayne Gray, and Jordan Marvakov (2021). *NBER-CES Manufacturing Industry Database (1958-2018, version 2021a)*.
- Bernanke, Ben S, Mark Gertler, and Simon Gilchrist (1999). “The financial accelerator in a quantitative business cycle framework”. In: *Handbook of macroeconomics* 1, pp. 1341–1393.
- Bianchi, Javier (2011). “Overborrowing and systemic externalities in the business cycle”. In: *American Economic Review* 101.7, pp. 3400–3426.
- Bianchi, Javier and Enrique G Mendoza (2018). “Optimal time-consistent macroprudential policy”. In: *Journal of Political Economy* 126.2, pp. 588–634.
- Bilal, Adrien (2023). “The geography of unemployment”. In: *The Quarterly Journal of Economics* 138.3, pp. 1507–1576.
- Borusyak, Kirill, Peter Hull, and Xavier Jaravel (2025). “A practical guide to shift-share instruments”. In: *Journal of Economic Perspectives* 39.1, pp. 181–204.
- Caliendo, Lorenzo, Maximiliano Dvorkin, and Fernando Parro (2019). “Trade and labor market dynamics: General equilibrium analysis of the china trade shock”. In: *Econometrica* 87.3, pp. 741–835.
- Caselli, Francesco et al. (2020). “Diversification through trade”. In: *The Quarterly Journal of Economics* 135.1, pp. 449–502.
- Costinot, Arnaud and Dave Donaldson (2012). “Ricardo’s theory of comparative advantage: old idea, new evidence”. In: *American Economic Review* 102.3, pp. 453–458.

- Costinot, Arnaud, Dave Donaldson, et al. (2015). “Comparative advantage and optimal trade policy”. In: *The Quarterly Journal of Economics* 130.2, pp. 659–702.
- Desmet, Klaus and Esteban Rossi-Hansberg (2014). “Spatial development”. In: *American Economic Review* 104.4, pp. 1211–1243.
- Dorn, David (2009). “Essays on inequality, spatial interaction, and the demand for skills”. PhD thesis. Verlag nicht ermittelbar.
- Eckert, Fabian (2019). “Growing apart: Tradable services and the fragmentation of the us economy”. In: *mimeograph, Yale University*.
- Eckert, Fabian, Teresa C Fort, et al. (2020). *Imputing Missing Values in the US Census Bureau’s County Business Patterns*. Tech. rep. National Bureau of Economic Research.
- Eckert, Fabian and Michael Peters (2022). *Spatial structural change*. Tech. rep. National Bureau of Economic Research.
- Fajgelbaum, Pablo, Eduardo Morales, et al. (2019). “State taxes and spatial misallocation”. In: *The Review of Economic Studies* 86.1, pp. 333–376.
- Fajgelbaum, Pablo and Stephen Redding (2022). “Trade, structural transformation, and development: Evidence from Argentina 1869–1914”. In: *Journal of political economy* 130.5, pp. 1249–1318.
- Gan, Jie (2007). “Collateral, debt capacity, and corporate investment: Evidence from a natural experiment”. In: *Journal of Financial Economics* 85.3, pp. 709–734.
- Ganong, Peter and Daniel Shoag (2017). “Why has regional income convergence in the US declined?” In: *Journal of Urban Economics* 102, pp. 76–90.
- Gertler, Mark and Peter Karadi (2011). “A model of unconventional monetary policy”. In: *Journal of monetary Economics* 58.1, pp. 17–34.
- Glaeser, Edward L et al. (1992). “Growth in cities”. In: *Journal of political economy* 100.6, pp. 1126–1152.
- Graham, John R, Mark T Leary, and Michael R Roberts (2015). “A century of capital structure: The leveraging of corporate America”. In: *Journal of financial economics* 118.3, pp. 658–683.
- Groth, Charlotta and Hashmat Khan (2010). “Investment adjustment costs: An empirical assessment”. In: *Journal of Money, Credit and Banking* 42.8, pp. 1469–1494.
- Hall, Robert E (2004). “Measuring factor adjustment costs”. In: *The Quarterly Journal of Economics* 119.3, pp. 899–927.
- Heathcote, Jonathan, Fabrizio Perri, and Giovanni L Violante (2010). “Unequal we stand: An empirical analysis of economic inequality in the United States, 1967–2006”. In: *Review of Economic dynamics* 13.1, pp. 15–51.
- (2020). “The rise of US earnings inequality: Does the cycle drive the trend?” In: *Review of economic dynamics* 37, S181–S204.

- Heathcote, Jonathan, Fabrizio Perri, Giovanni L Violante, and Lichen Zhang (2023). “More unequal we stand? Inequality dynamics in the United States, 1967–2021”. In: *Review of Economic Dynamics* 50, pp. 235–266.
- Heblich, Stephan et al. (2025). *The death and life of great British cities*. Tech. rep. National Bureau of Economic Research.
- Imbs, Jean and Romain Wacziarg (2003). “Stages of diversification”. In: *American economic review* 93.1, pp. 63–86.
- Jacobs, Jane (1969). “Strategies for helping cities”. In: *The American Economic Review* 59.4, pp. 652–656.
- (1985). *Cities and the wealth of nations: Principles of economic life*. Vintage.
- Kiyotaki, Nobuhiro and John Moore (1997). “Credit cycles”. In: *Journal of political economy* 105.2, pp. 211–248.
- Mendoza, Enrique G (2010). “Sudden stops, financial crises, and leverage”. In: *American Economic Review* 100.5, pp. 1941–1966.
- Moffitt, Robert and Sisi Zhang (2018). “Income volatility and the PSID: Past research and new results”. In: *AEA Papers and Proceedings*. Vol. 108. American Economic Association 2014 Broadway, Suite 305, Nashville, TN 37203, pp. 277–280.
- Moretti, Enrico (2010). “Local multipliers”. In: *American Economic Review* 100.2, pp. 373–377.
- Moroney, John R and James M Walker (1966). “A regional test of the Heckscher-Ohlin hypothesis”. In: *Journal of Political Economy* 74.6, pp. 573–586.
- Morris-Levenson, Joshua (2022). “The Origins of Regional Specialization”. PhD thesis. The University of Chicago.
- Nagy, Dávid Krisztián (2023). “Hinterlands, city formation and growth: Evidence from the US westward expansion”. In: *Review of Economic Studies* 90.6, pp. 3238–3281.
- Walsh, Conor (2023). “The Startup Multiplier”. In.

A Empirical Appendix

A.1 Top-coding CPS data

Top-coding is an important issue to address in the CPS for measuring income at the top of the income distribution. I follow Heathcote, Perri, and Violante (2010) in dealing with top-coded observations by assuming the underlying distribution of income is Pareto, and follow as suggestion from David Domeij to extrapolate top-coded observations based on this assumption. Since regional variation is the relevant factor in this paper, I deviate from the authors by defining the distribution at the state-level rather than the country-level. A more detailed explanation of the top-coding process is given by Heathcote, Perri, and Violante (2020).

A.2 Industry details

Table (3) details the employment shares of 17 major industries for the years 1950, 1990, and 2020. These aggregate sectors are constructed from 865 detailed 3-digit industry classifications sourced from the U.S. Decennial Census data. The table further categorizes each industry as either tradable or nontradable. This distinction is based on a qualitative assessment of whether an industry's output primarily competes within a local market or on a broader national scale. Tradable industries are considered those whose output can be readily sold and consumed far from its point of production; this sector includes industries like Agriculture, Mining, and nearly all forms of Manufacturing. Nontradable industries, conversely, primarily serve local demand with output that is consumed locally; this sector is composed mainly of services, such as Construction, Retail Trade, Education, and Personal Services. This conceptual distinction is useful for contextualizing the patterns of specialization documented in the main text.

	Industry	1950	1990	2020	Tradable
1	Agriculture	20.71	3.61	3.46	Yes
2	Business Services	2.96	4.43	7.61	Yes
3	Communication	0.61	1.52	1.36	No
4	Construction	8.75	9.98	11.91	No
5	Durable	13.53	15.88	10.77	Yes
6	Entertainment	0.66	1.06	1.28	No
7	Finance	2.20	4.47	4.79	No
8	Mining	3.99	1.90	1.82	Yes
9	Nondurable	9.48	8.64	5.77	Yes
10	Personal Services	2.37	1.39	1.60	No
11	Routine Prof. Serv.	4.39	11.26	13.19	No
12	Non-routine Prof. Serv.	0.37	2.02	3.33	Yes
13	Public	4.67	7.96	6.98	No
14	Retail	11.84	11.15	13.26	No
15	Transportation	8.09	6.61	6.91	Yes
16	Utilities	1.80	2.53	2.34	No
17	Wholesale	3.59	5.60	3.63	Yes

Table 3: Employment shares

A.3 Fact 1: Robustness and Extensions

In this section, I provide a range of robustness and extension exercises on Fact 1 as described in section (2).

A.3.1 Regression Table: Equation (5)

Table (4) shows the regression results from equation (5). The control variables are the following. Specialization is given by the Gini coefficient on income shares by 3-digit CPS industry. I decompose specialization further into tradable and non-tradable industries. All other variables are included at their 1950 level. The exposure to structural change is captured by the shift-share instrument \hat{g} . High-skill share is the share of employed workers with at least one year of higher education. The old-age dependency ratio is the share of workers younger than 25 over workers older than 25.

The results presented in Table (4) provide a detailed empirical foundation for Fact 1. Columns (1) and (3) directly test the specialization trade-off highlighted in the main text. The coefficient on the overall specialization is negative for long-run growth (-0.233), while being positive for initial 1950 income per capita (0.844). On average, more specialized commuting zones in 1950 were initially richer but experienced slower growth over the subsequent 70 years.

Columns (2) and (4) extend this finding by decomposing specialization into its tradable and nontradable components as defined in Table (5). This decomposition reveals that the trade-off is driven almost exclusively by specialization in tradable industries. A higher concentration in tradable sectors is associated with slower long-run growth (-0.151) and higher initial income (0.110). In contrast, the coefficients for specialization in nontradable industries are insignificantly different from zero, suggesting that concentration in local services and similar sectors does not exhibit the same trade-off. Intuitively, whether a region has disproportionately many hairdressers cannot predict a regions expected growth and relative income. If, however, all tradable output is generated in a single tradable sector (e.g. cash registers as in Dayton, Ohio) appears to be a relevant predictor for future growth.

Across all four specifications, the control variables are largely significant and informative. The highly significant negative coefficient on the initial log income p.c. in the growth regressions provides strong evidence of conditional convergence, indicating that poorer regions tended to grow faster. Human capital, measured by the high-skill labor share, is a powerful predictor of both higher initial income and faster subsequent growth. Similarly, the 1950 population is positively correlated with both outcomes, consistent with the presence of agglomeration economies. The shift-share instrument for structural change, \hat{g} , exhibits a negative coefficient across all models, suggesting that regions with an industrial mix that was predicted to grow based on national trends tended to have lower initial incomes and experience slower growth, once other local characteristics are controlled for. Overall, the models demonstrate substantial explanatory power, with an adjusted R-squared of approximately 0.54 for the full growth models.

	1950-2020 Growth		1950 Income p.c.	
	(1)	(2)	(3)	(4)
Specialization	-0.233*		0.844***	
	(0.0901)		(0.084)	
Tradable		-0.151***		0.110**
		(0.0388)		(0.0423)
Non-tradable		0.632		-0.43
		(0.294)		(0.456)
1950 measures:				
\hat{g}	-0.180***	-0.133*	-0.187**	-0.319***
	(0.0471)	(0.0521)	(0.058)	(0.0631)
log income p.c.	-0.868***	-0.885***		
	(0.0339)	(0.0323)		
High-skill labor share	1.435***	1.618***	6.042***	5.692***
	(0.41)	(0.418)	(0.402)	(0.431)
Old-age dependency ratio	0.0145**	0.0120*	-0.0187***	-0.0230***
	(0.00532)	(0.00553)	(0.00484)	(0.00526)
Female labor share	0.984***	0.965***	0.0754	0.283
	(0.167)	(0.184)	(0.164)	(0.187)
Population	170.6***	163.0***	136.8***	152.0***
	(35.55)	(33.46)	(25.75)	(31.66)
N	722	722	722	722
adj. R-sq	0.538	0.544	0.41	0.344

Table 4: Regression table of regression (5)

A.3.2 Regression Table: Equation (5) across different macro industries

This section investigates the heterogeneity of the specialization trade-off across different sectors of the economy. Table (5) presents the results, where the aggregate specialization from equation (5) is replaced by specialization within six major industries simultaneously. Note that these results are quantitatively similar to those obtained when estimating the equation for each industry individually.

The estimates reveal that the trade-off is not uniform and is heavily concentrated in specific industries. The pattern is most pronounced for Manufacturing and Wholesale Trade. Specialization in Manufacturing is associated with significantly lower long-run growth (-1.086) but higher initial income (2.296). This effect is even stronger and more precisely estimated for Wholesale Trade, which shows the largest negative coefficient on growth (-2.356) and a strong positive association with 1950 income (2.992).

In contrast, other sectors show different or insignificant patterns. Specialization in Retail and Transportation was associated with higher initial income but had no statistically significant relationship with long-run growth. Interestingly, a higher concentration in Services in 1950 is linked to significantly lower initial income levels, while specialization in Agriculture shows no significant association with either outcome. These results strongly suggest that the aggregate specialization trade-off documented in the main text is primarily driven by concentration in goods-producing and distributing sectors.

The standard set of control variables, including initial income, high-skill share, and population, remain highly significant across both columns, and their coefficients are quantitatively similar to those in the main specification (Table 4). The relative size of the sectors n 1950 is shown in Table (3).

	1950-2020 Growth	1950 Income level
	(1)	(2)
Specialization in		
Manufacturing	-1.086** (0.373)	2.296*** (0.488)
Services	1.441 (1.201)	-5.386** (1.776)
Agriculture	-0.0653 (0.191)	0.35 (0.241)
Transportation	0.397 (0.912)	2.071* (0.894)
Wholesale	-2.356*** (0.698)	2.992** (0.994)
Retail	-0.747 (0.764)	3.404*** (0.64)
1950 measures:		
\hat{g}	-0.249** (0.0836)	0.0241 (0.11)
log income p.c.	-0.863*** (0.0345)	
High-skill labor share	1.380*** (0.411)	5.687*** (0.399)
Old-age dependency ratio	0.0163** (0.00542)	-0.0228*** (0.00492)
Female labor share	1.137*** (0.186)	-0.0526 (0.194)
Population	165.7***	149.6***
N	722	722
adj. R-sq	0.54	0.399

Table 5: Regression table of regression (5) across different industries

A.3.3 Regression Table: Equation (5) with the Herfindahl index

Table(6) shows the regression results using the Herfindahl-Hirschman Index (HHI) as a measure of specialization. The results are in line with the baseline results: a greater specialization in 1950 is related to higher per capita income in 1950, but lower growth between 1950-2020. While both the HHI and the Gini coefficient measure concentration, they differ in their construction and sensitivity. The HHI is calculated as the sum of the squared income shares of all industries in a region. This method gives disproportionately more weight to the largest industries, making it particularly sensitive to the presence of one or two dominant sectors. In contrast, the Gini coefficient measures the inequality across the entire distribution of industry shares and is less influenced by extreme values. It provides a broader assessment of how evenly distributed economic activity is.

	1950-2020 Growth	1950 Income level
	(1)	(2)
Specialization	-0.212*	0.933***
	(0.122)	(0.134)
\hat{g}	-0.169***	-0.233**
	(0.0470)	(0.064)
log income	-0.886***	
	(0.0328)	
Highhh-skill share	1.482***	6.351***
	(0.424)	(0.436)
Old-age dependency	0.0149**	-0.0213***
	(0.00532)	(0.00512)
Female share	1.04***	-0.172
	(0.167)	(0.179)
Population	172.7***	136.7***
	(35.77)	(25.67)
N	722	722
adj. R-sq	0.535	0.375

Table 6: Regression table of regression (5) with HHI

A.3.4 Regression Table: Equation (5) at different horizons

This section explores the temporal dynamics of the specialization trade-off by running a series of dynamic panel regressions. Instead of a single cross-section, here I regress future income per capita growth over a specific horizon (k years) on the level of specialization at the beginning of that period (in year $t - h$). The coefficient of interest β^h is estimated

from the following regression:

$$y_{c,t} - y_{c,t-h} = \alpha^h + \beta^h \cdot Gini_{c,t-h} + \delta \cdot \hat{g}_{c,t-h} + \gamma' \cdot Z_{c,t-h} + \epsilon_{c,t-h} \quad (30)$$

where all controls correspond to the controls in equation (5) at horizon $t - h$. Table (7) reports the effect of specialization on income growth over different time horizons. These findings provide two crucial insights. First, the adverse effects of tradable specialization are not immediate but emerge and accumulate over decades, consistent with a story of slowing adaptation or declining dynamism in economies heavily reliant on a narrow set of tradable industries. The table shows that the adverse effect of specialization on growth appears after a 20-year horizon. Second, the negative long-run consequence of specialization is driven specifically by concentration in tradable industries.

	Income pc growth						
	10-year (1)	20-year (2)	30-year (3)	40-year (4)	50-year (5)	60-year (6)	70-year (7)
Trad. Specialization (t-10)	0.00152 (-0.025)						
Trad. Specialization (t-20)		-0.0747*** (-0.0209)					
Trad. Specialization (t-30)			-0.106*** (-0.0254)				
Trad. Specialization (t-40)				-0.162*** (-0.0293)			
Trad. Specialization (t-50)					-0.1420** (-0.0147)		
Trad. Specialization (t-60)						-0.152** (-0.0347)	
Trad. Specialization (t-70)							-0.154*** (-0.04)
N	3528	3563	2842	2123	1403	1007	700
adj. R-sq	0.101	0.113	0.152	0.219	0.308	0.403	0.549

Table 7: Regression table: Specialization on growth at different horizons

A.3.5 Map of exposure to structural change

Figure (12) displays the geographical distribution of predicted income growth, \hat{g}_c , across all U.S. commuting zones (CZs). As defined in equation (2), this variable captures the long-run growth (1950-2020) that a CZ was structurally exposed to, based purely on its initial 1950 composition of 1-digit industries and the subsequent national growth rates of those industries. The map reveals stark regional patterns that reflect the major structural transformations in the U.S. economy over the latter half of the 20th century. Regions with high predicted growth (indicated by darker shades) are heavily concentrated in the Sun Belt and the West Coast. These areas had a larger initial employment share in

sectors that experienced high national growth, such as services and, later, technology. In contrast, regions with low or even negative predicted growth (lighter shades) are prominent throughout the Rust Belt, the industrial Midwest, and parts of the Great Plains. These CZs were historically specialized in manufacturing and agriculture, sectors that experienced significant relative decline or slower growth at the national level. The map thus provides a clear visual representation of the structural economic headwinds and tailwinds that different regions faced, underscoring the necessity of including \hat{g}_c as a control in equation (5) to isolate the distinct economic effects of industrial specialization.

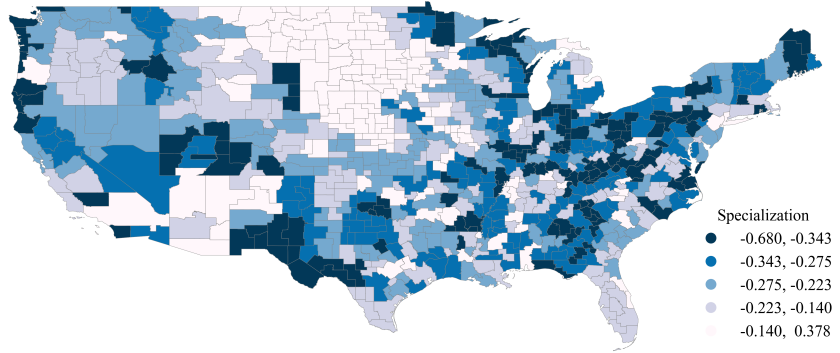


Figure 12: Commuting Zones by 1950 exposure to structural change

Notes: This figure shows a map of commuting zones binned by their 1950 estimate of \hat{g} from equation (2).

A.3.6 Specialization trade-off at 20-year horizon

Figure (13) plots coefficients from two separate panel regressions estimated at a 20-year horizon. I show the 20-year horizon as the specialization trade-off appears at that horizon as shown above. Instead of a single linear coefficient, the effect of specialization is captured using dummy variables for 20 quantiles of the specialization Gini. The coefficients are estimated from the following regression:

$$y_{c,t-20} = \sum_{k=2}^{20} [\beta_k \cdot D_{k,c,t-20} + \delta \cdot \hat{g}_{k,c,t-20} + \gamma' \cdot Z_{k,c,t-20} + \epsilon_{k,c,t}] \quad (31)$$

where $D_{k,c,t-20}$ is a binary dummy equal to one if a commuting zone falls into the k -th quantile of specialization at time $t - 20$. The figure illustrates the specialization trade-off: The left panel shows an upward-sloping relationship, indicating that commuting zones in higher quantiles of specialization have systematically higher initial income per capita. The

right panel shows a downward-sloping relationship, meaning regions in higher specialization quantiles experience significantly lower income growth over the subsequent 20 years. This confirms that the benefits of specialization in terms of higher income are contemporaneous, while the costs in terms of lower growth emerge over longer horizons.

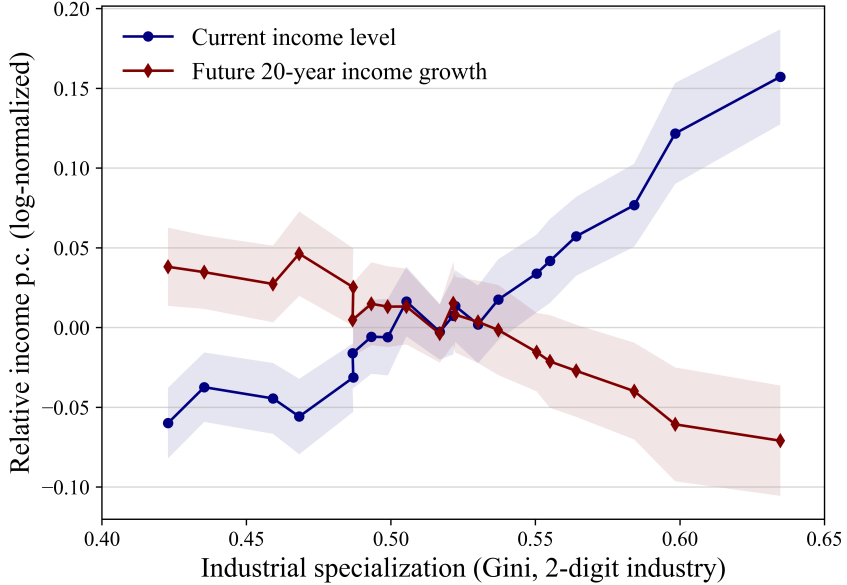


Figure 13: Industrial specialization, relative income and long-run growth

Notes: This figure plots the coefficients of regressions of 10-year commuting zone-level income growth and initial per capita income on dummies for 20 quantiles of the initial specialization, for the period 1950-2020. Specialization is computed as the Gini coefficient on 3-digit level industry income shares. 95% confidence intervals are shaded.

A.3.7 Map of regional specialization

This section provides a visual overview of how the geography of regional specialization has evolved in the United States over the last 70 years. The two figures map the concentration of economic activity across U.S. commuting zones at the beginning and end of the analysis period, grouping regions into five quintiles based on their specialization Gini coefficient, where darker shades represent a higher degree of industrial specialization.

The 1950 map shows that high levels of specialization were concentrated in the nation's industrial heartland. The darkest shades, indicating the most specialized regions, are located almost exclusively in the Rust Belt and the industrial Midwest, along with some areas in the Southeast. This pattern reflects an economy where regional dominance was defined by heavy manufacturing and specific industries, such as automobile production in and around Detroit, steel manufacturing in Pennsylvania, and textiles in the Carolinas.

By 2020, the economic landscape has transformed entirely. The once-specialized Rust

Belt now exhibits significantly lower levels of industrial concentration. Instead, the new centers of high specialization are found predominantly on the East and West Coasts. This modern pattern is driven by knowledge-intensive and high-skill service industries. For instance, the highest levels of specialization are now seen in the technology sector of the San Francisco Bay Area, the financial and business services of the New York metropolitan area, and the entertainment industry of Los Angeles. Together, the two maps visually narrate the profound economic shift from a manufacturing-based economy to a knowledge-and service-based one.

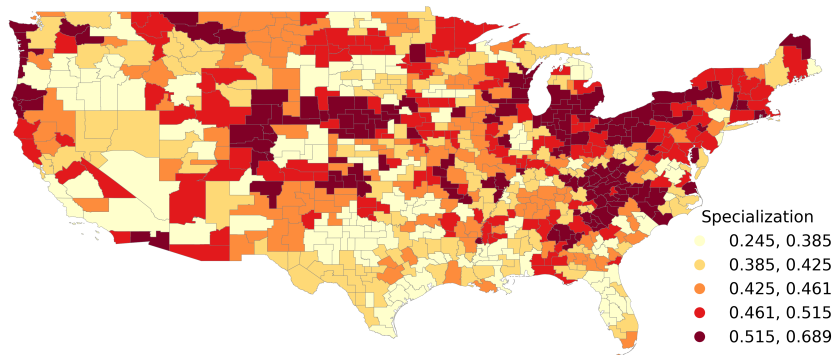


Figure 14: Commuting Zones by 1950 specialization

Notes: This figure shows a map of commuting zones binned by 1950 regional specialization as measured by the Gini coefficient on 1950 income shares by 3-digit industry.

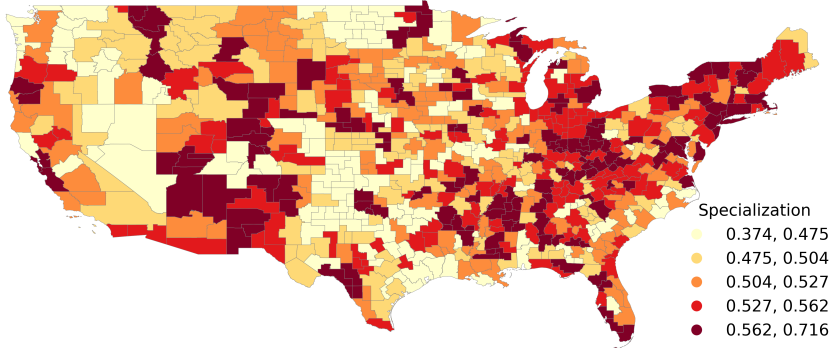


Figure 15: Commuting Zones by 2020 specialization

Notes: This figure shows a map of commuting zones binned by 2020 regional specialization as measured by the Gini coefficient on 2020 income shares by 3-digit industry.

A.3.8 Convergence and regional specialization

This section documents the evolution of regional income inequality in the U.S. since 1950, analyzing data at both the state and commuting zone levels. The analysis combines U.S. Census data for commuting zones with state-level data from the Bureau of Economic Analysis and housing value data from the NHGIS. Spatial dispersion is measured using the coefficient of variation of earnings per worker. To account for differences in local purchasing power, nominal income at the commuting zone level is deflated using a local housing price index, which serves as a proxy for the local price level.

To adjust for local price levels, I construct a housing price index for each commuting zone (CZ) and year using binned housing value data from the NHGIS. The process involves three steps. First, for each housing value bin provided in the data, I calculate a midpoint value. Second, for each CZ in a given year, I compute the mean housing value by taking a weighted average of these midpoints, where the weights are the number of housing units in each respective bin. Finally, the housing price index is created by taking the logarithm of this mean value. This creates a consistent price index across time and space.

Figure (16) plots this measure of dispersion over time, illustrating a well-documented two-phase pattern. From 1950 until the early 1990s, the U.S. experienced a period of strong regional convergence, where the income gap between poorer and richer regions steadily narrowed, a finding consistent with the literature established by authors such as Barro and Sala-i-Martin (1992). However, since the 1990s, this trend has not only stalled but has reversed, leading to a new era of regional divergence where spatial income dispersion has

increased, in some cases reaching levels higher than in the initial period.

This recent divergence can be driven by two distinct dynamics. One possibility is a persistent income hierarchy, where initially rich regions simply began growing faster than their poorer counterparts, thus increasing the distance between them without significant changes in their relative income rankings. An alternative explanation involves rank reversals, where the fortunes of regions have shifted over time, with some once-prosperous areas declining while other, previously poorer regions have risen. This is illustrated by the divergent paths of Dayton, Ohio, and Rochester, Minnesota, in Figure (1).

The theory developed in this paper offers a mechanism that can explain aspects of the latter story. The model captures how formerly rich regions, characterized by a high degree of specialization in specific industries, can experience long-term decline when those industries falter. This lock-in effect contrasts with the trajectory of other regions that, despite potentially lower initial specialization, possessed a more diverse industrial portfolio that facilitated greater adaptability and long-run growth.

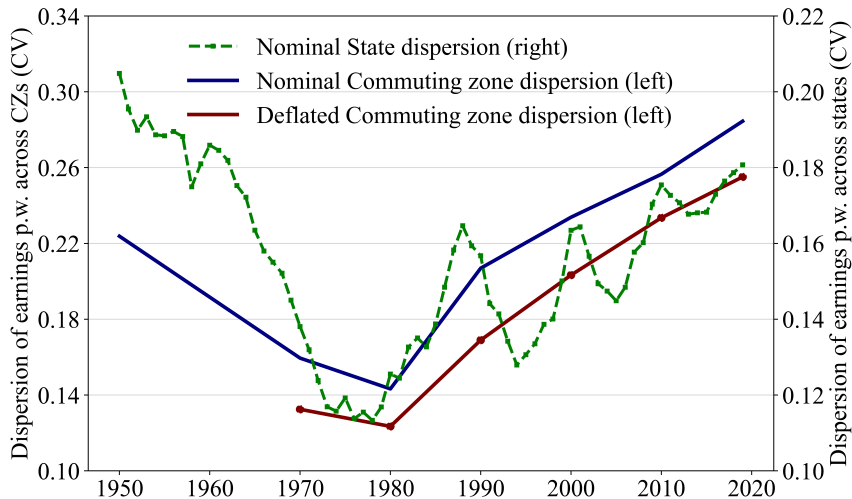


Figure 16: Dispersion of income p.c. across labor markets

Notes: This figure shows a spatial dispersion of per capita income across the U.S. since 1950.

A.4 Fact 2: Robustness and Extensions

In this section, I provide a range of robustness and extension exercises on Fact 2 as described in section (2).

A.4.1 Parametric specification

This section provides a parametric comparison to assess whether a standard linear model can adequately capture the relationship between regional specialization and income. For this purpose, I perform a simple Ordinary Least Squares (OLS) regression of log-normalized specialization on relative per capita income using the following specification:

$$Gini_{c,t} = \alpha + \beta y_{c,t} + \epsilon_{c,t}$$

Figure (17) plots the linear fit derived from this regression against relative income, along with the 95 percent confidence interval. As is evident from the figure, the OLS model imposes a constant linear relationship between the two variables. This simple functional form is unable to capture the non-linear, S-shaped pattern identified in the main analysis, thereby motivating the use of more flexible non-parametric methods to characterize this relationship accurately.

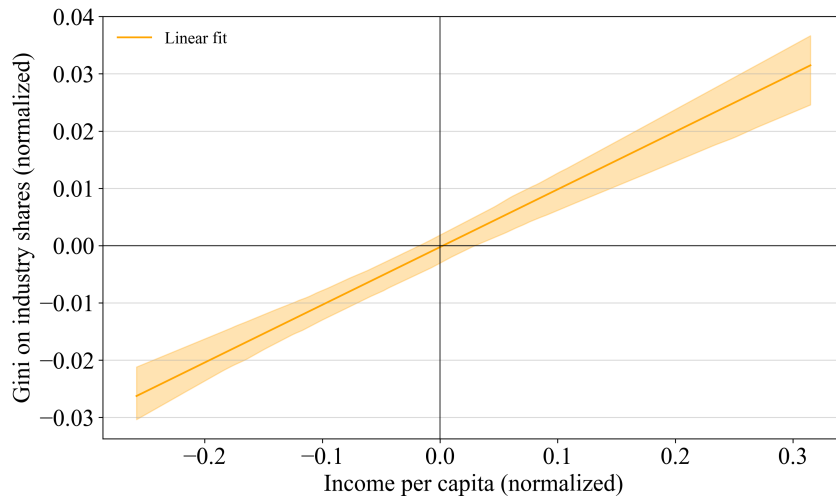


Figure 17: OLS estimate: Specialization vs. per capita income

Notes: The figure plots fitted values of normalized relative specialization against relative income. 95% bootstrapped confidence interval shown as a shaded area.

A.4.2 Specialization change on Change

This section provides a dynamic test of the relationship between specialization and income by examining how changes in one are related to changes in the other over time. To analyze this relationship in first differences, I estimate a 'change-on-change' regression for various horizons (h) using the following specification:

$$\log Gini_{c,t} - \log Gini_{c,t-h} = \alpha + \beta^h (\log y_{c,t} - \log y_{c,t-h}) + \gamma^h \log y_{c,t-h} + \epsilon_{c,t} \quad (32)$$

Here, the dependent variable is the log change in specialization over an h -year period. The main independent variable is the log change in per capita income over the same period, and the model also controls for the initial income level to account for any convergence effects.

Table (8) reports the estimates for the coefficient on the change in income, β^h . The key result is that the coefficient is positive and statistically significant across all time horizons, from 10 to 60 years. This indicates that regions experiencing faster income growth are also, on average, the ones whose economies become more specialized.

This finding provides strong dynamic support for Fact 2. The S-shaped relationship described in the main text implies that as regions develop and their incomes rise, their specialization levels also tend to increase. This regression confirms that very pattern by showing that periods of growth coincide with periods of rising specialization, demonstrating that the cross-sectional relationship holds dynamically within regions over time.

		Change in Specialization					
		10-year (1)	20-year (2)	30-year (3)	40-year (4)	50-year (5)	60-year (6)
Change in income pc.c (t-10)	0.313*** (0.0255)						
		0.159*** (0.0321)					
			0.264*** (0.0385)				
				0.545*** (0.0422)			
					0.512** (0.0571)		
						0.393** (0.0487)	
	N	4332	3610	2888	2166	1444	722
adj. R-sq		0.064	0.047	0.087	0.275	0.327	0.113

Table 8: Regression table: Specialization change on income change

A.5 Fact 3: Robustness and Extensions

In this section, I provide a range of robustness and extension exercises on Fact 3 as described in section (2).

A.5.1 Persistence of Specialization at the regional level

This section evaluates the persistence of regional specialization over time using a rank-rank regression approach. For each period, commuting zones are ranked based on their

specialization level, as measured by the log Gini coefficient of 3-digit industry income shares. The rank of a commuting zone at time t is then regressed on its rank at time $t - h$ for various horizons h , according to the following specification:

$$\text{Rank}_{c,t} = \alpha^h + \beta^h \cdot \text{Rank}_{c,t-h} + \epsilon_{c,t} \quad (33)$$

The coefficient of interest, β^h , is the rank-rank elasticity, which measures the degree of persistence. A value of one indicates perfect persistence, while a value of zero implies no relationship between past and future rankings.

Figure (18) plots the estimated elasticity β^h for horizons up to 70 years. The results show that regional specialization is highly persistent in the short run, but this persistence decays steadily over time. For instance, the estimate for a 60-year horizon is approximately 0.2. This implies that a 10 percent higher specialization rank is associated with only a 2 percent higher rank 60 years later. This demonstrates that while specialization rankings are sticky in the short to medium term, there is considerable mobility in the regional specialization hierarchy over the long run.

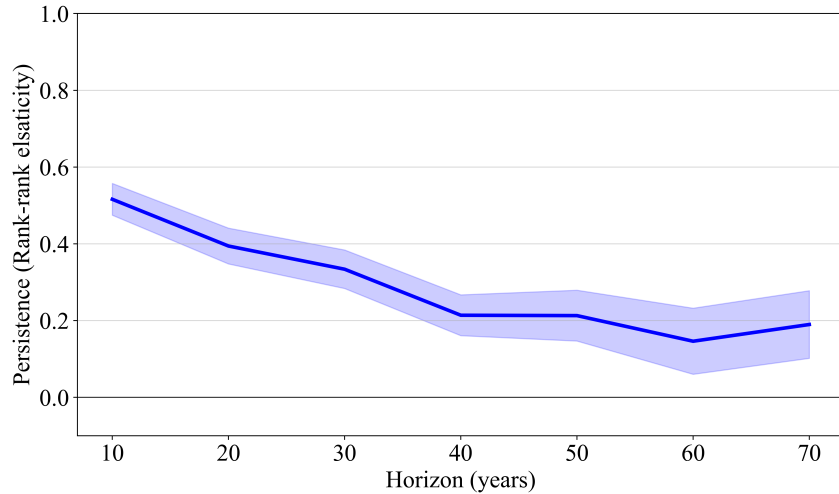


Figure 18: Persistence at the regional level

Notes: Figure (18) shows the rank-rank elasticity of regional specialization over a 70-year horizon, estimated from the regression in equation (5). The shaded area represents the 90% confidence interval.

A.5.2 Persistence of comparative advantages over time

The persistence of revealed comparative advantages (RCA) can be computed using the location-quotient - the ranking of sectors comparative advantage in a state over time. The revealed comparative advantage for each sector i in state c is given by $RCA_{i,c} = \left(\frac{X_{c,i}}{\sum_{i \in I} X_{c,i}} / \frac{X_{US,i}}{\sum_{i \in I} X_{US,i}} \right)$. Second, one can rank $RCA_{i,c}$ for every state-year and auto-regress

it over different horizons as follows:

$$Rank_{c,i,t} = \alpha + \rho_{c,h} Rank_{c,i,t-h} + \epsilon_{c,i,t}$$

The following table shows the regression results. The ranking is highly persistence over short, medium and long-run horizons.

Horizon	1	5	10	20
Persistence	0.961*** (0.002)	0.8962*** (0.003)	0.839*** (0.004)	0.8148*** (0.025)

Table 9: RCA persistence

A.6 Calibration: Further details

A.6.1 Agglomeration by industry

Table (10) reports the parameters for industry-specific agglomeration economies, ξ_i , which are used to calibrate the model in the main text. The estimates are taken directly from the study by Bartelme et al. (2019).

In this context, the parameter ξ_i represents the elasticity of an industry's productivity with respect to its own local size or density. For example, the value of 0.16 for the Food, Beverages and Tobacco industry implies that a 10 percent increase in the local scale of this sector is associated with a 1.6 percent increase in its productivity. These parameters are intended to capture the positive technological externalities that arise when firms in the same industry cluster together.

The original authors estimate these sector-level economies of scale using annual international trade data from 1995 to 2010 for the 15 2-digit manufacturing industries shown. The estimates exhibit considerable variation across sectors, ranging from a low of 0.07 for Coke and Petroleum Products to a high of 0.25 for Rubber and Plastics, highlighting that the strength of agglomeration forces is highly industry-specific.

Industry	ξ_i
Food, Beverages and Tobacco	0.16
Textiles	0.12
Wood Products	0.11
Paper Products	0.11
Coke/ Petroleum Products	0.07
Chemicals	0.2
Rubber and Plastics	0.25
Mineral Products	0.13
Basic Metals	0.11
Fabricated Metals	0.13
Machinery and Equipment	0.13
Computers and Electronics	0.09
Electrical Machinery	0.09
Motor Vehicles	0.15
Other Transport Equipment	0.16

Table 10: Agglomeration parameter by industry

A.6.2 Capital adjustment costs by industry

This section details the parameters for industry-specific capital adjustment costs, Φ_i , used in the main analysis. Table (11) reports estimates from two empirical studies, Groth and Khan (2010) and Hall (2004).

These parameters govern the magnitude of convex costs that firms incur when they change their capital stock. The specific functional form for these costs used in this paper is:

$$\Phi_i(k_{i,t}, k_{i,t+1}) = \frac{\Phi_i}{2} \left(\frac{k_{i,t+1}}{k_{i,t}} - 1 - \delta_i \right)^2 k_{i,t} \quad \Phi_i \geq 0 \quad \forall i \quad (34)$$

with depreciation rate δ_i . In this specification, a larger value of Φ_i implies that it is more costly for firms in industry i to rapidly adjust their capital stock.

The parameters from the cited studies were originally estimated from the first-order conditions of firm investment problems, using annual U.S. industry and firm-level data from 1948 to 2001. The parameters for capital adjustment costs reported in Table (11) reveal two key patterns with important implications for the model. First, the cost of adjusting capital is highly heterogeneous across sectors. The estimates vary substantially from one industry to another, and the two cited studies sometimes provide different rankings. For instance, the parameter for fabricated metals is 50% higher than for wooden products. This wide variation underscores the importance of using industry-specific parameters in a multi-sector model rather than a single, aggregate value.

Second, for many industries, the estimated parameters are small and often statistically insignificant from zero. This suggests that for a significant portion of the manufacturing sector, the physical costs of investment play a relatively minor role. This finding is consistent with the broader empirical literature, which often documents small estimated adjustment costs (see, e.g., Hall (2004)). For the scope of this paper, this implies that these physical frictions are likely not the primary driver of the strong persistence of specialization observed in the data. Other economic mechanisms, such as financial frictions or agglomeration economies, must therefore be at play.

Industry	Groth & Khan (2007)	Hall (2004)
Food, Beverages and Tobacco	0.01	-0.43
Textiles	3.26	-0.58
Wood Products	0.26	-0.22
Paper Products	0	-0.15
Coke/ Petroleum Products	-0.04	0.26
Chemicals	-0.08	-0.02
Rubber and Plastics	-0.2	-1.75
Mineral Products	0.1	0
Basic Metals	0.15	-0.06
Fabricated Metals	0.37	0.27
Machinery and Equipment	0.22	-0.92
Computers and Electronics	-0.01	0.38
Electrical Machinery	-0.01	-0.09
Motor Vehicles	0.25	0.4
Other Transport Equipment	-0.06	3.02

Table 11: Adjustment cost parameter by industry

B Theory Appendix

B.1 Cross-derivatives in Planner optimality conditions

In recursive form, the cross-derivative of the bond decision and capital allocation decision rules are given by:

$$\Omega_i^B = \frac{1}{R} \left[\frac{\partial u'(\mathcal{C}(b', \mathcal{K}', \mathcal{Z}'))}{\partial b'} (\mathcal{Q}(b', \mathcal{K}', \mathcal{Z}') + \alpha z'_i k_i'^{\xi_i + \alpha - 1} - \phi_{1i}) + u'(\mathcal{C}(b', \mathcal{K}', \mathcal{Z}')) \left(\frac{\partial \mathcal{Q}(b', \mathcal{K}', \mathcal{Z}')}{\partial b'} - \frac{\partial \phi_{1i}}{\partial b'} \right) + \theta \left(\frac{\partial q'}{\partial b'} \eta' - \frac{\partial \eta'}{\partial b'} \mathcal{Q}(b', \mathcal{K}', \mathcal{Z}') \right) \right] \quad (35)$$

$$\begin{aligned} \Omega_i^K = & -u'(c)\phi_{22,i} + \frac{1}{R} \left[\frac{\partial u'(\mathcal{C}(b', \mathcal{K}', \mathcal{Z}'))}{\partial k_i'} (\mathcal{Q}(b', \mathcal{K}', \mathcal{Z}') + \alpha z'_i k_i'^{\xi_i + \alpha - 1} - \phi_{1i}) \right. \\ & + u'(\mathcal{C}(b', \mathcal{K}', \mathcal{Z}')) \left(\frac{\partial \mathcal{Q}(b', \mathcal{K}', \mathcal{Z}')}{\partial k_i'} + (\xi_i + \alpha - 1) \alpha z'_i k_i'^{\xi_i + \alpha - 2} - \phi_{11,i} - \phi_{12,i} \frac{\partial k_i''}{\partial k_i'} \right) \\ & \left. + \theta \left(\frac{\partial q'}{\partial k_i'} \eta' - \frac{\partial \eta'}{\partial k_i'} \mathcal{Q}(b', \mathcal{K}', \mathcal{Z}') \right) \right] \end{aligned} \quad (36)$$

Equation (35) captures the effects of a change in bond holdings today on the current and future price of capital through the cross-derivatives of the implementability constraints. It consists of three components. The first, captures how an extra unit of b_{t+1} affects future consumption and thus the discounting of future asset returns through the marginal utility. The second includes the effects by which b_{t+1} alters the marginal return of capital (i.e. dividends) in industry i . The third shows how it affects the future tightness of the collateral constraint.

Condition (36) captures the effects of a change in capital allocated to industry i on the current and future price of capital through the cross-derivatives of the implementability constraints. It consists of four terms. The first is the curvature on the adjustment costs $\phi_{22,i}$. The second, captures the effect of an increase in $k_{i,t+1}$ on future consumption, thus affecting the discounting of future asset returns. The third captures the effect by which a higher $k_{i,t+1}$ alters future dividends. The fourth consists both of the curvature of the production function as well as the agglomeration externality ξ_i . The final term shows how an additional unit of capital loosens the future collateral constraint.

B.2 Proof: Proposition 1

Proposition 1 (Decentralization with taxes and subsidies). *The constrained-efficient equilibrium can be decentralized with a state-contingent tax on debt, and industry-specific tax and subsidies with tax revenue rebated as a lump-sum transfer and the tax rates set to*

satisfy:

$$1 + \tau_t^B = \frac{1}{\mathbb{E}_t[u'(t+1)]} \left[\sum_i \delta_{i,t} \Omega_{i,t+1}^B - \frac{u''(t+1)}{u'(t+1)} \theta \eta_{t+1} q_{t+1} - u''(t+1) \sum_i \delta_{i,t+1} \phi_{i,t+1}^2 \right] \\ + \frac{1}{\beta R_t \mathbb{E}_t[u'(t+1)]} \mathbb{E}_t \left[\frac{u''(t)}{u'(t)} \theta \eta_t q_t + u''(t) \sum_i \delta_{i,t} \phi_{i,t}^2 \right] \quad (37)$$

$$1 + \tau_{i,t}^K = \frac{1}{\mathbb{E}_t[\alpha z_{i,t+1} k_{i,t+1}^{\alpha+\xi_i-1}]} \left[\left(u'(t+1) - \frac{u''(t+1)}{u'(t+1)} \theta \eta_{t+1} q_{t+1} - u''(t+1) \sum_i \delta_{i,t+1} \phi_{i,t+1} \right) \right. \\ \left. ((\alpha + \xi_i) z_{i,t+1} k_{i,t+1}^{\alpha+\xi_i-1} - \phi_{i,t+1}^1) + \sum_i \delta_{i,t} \Omega_{i,t+1}^K \right. \\ \left. - u'(t)(q_{t+1} - \phi_{i,t}^1) - \theta \eta_{t+1} q_{t+1} \right] \\ + \frac{1}{\beta \mathbb{E}_t[\alpha z_{i,t+1} k_{i,t+1}^{\alpha+\xi_i-1}]} \left(u'(t) q_t + \Xi + \phi_{i,t}^2 u''(t) \sum_i \delta_{i,t} \phi_{i,t}^2 \right) \quad (38)$$

where the arguments of the functions have been shorthanded as dates to keep the expression simple.

Define the taxes as:

$$1 + \tau_t^B = \frac{1}{\mathbb{E}_t[u'(t+1)]} \left[\sum_i \delta_{i,t} \Omega_{i,t+1}^B - \frac{u''(t+1)}{u'(t+1)} \theta \eta_{t+1} q_{t+1} - u''(t+1) \sum_i \delta_{i,t+1} \phi_{i,t+1}^2 \right] \\ + \frac{1}{\beta R_t \mathbb{E}_t[u'(t+1)]} \mathbb{E}_t \left[\frac{u''(t)}{u'(t)} \theta \eta_t q_t + u''(t) \sum_i \delta_{i,t} \phi_{i,t}^2 \right] \quad (39)$$

$$1 + \tau_{i,t}^K = \frac{1}{\mathbb{E}_t[\alpha z_{i,t+1} k_{i,t+1}^{\alpha+\xi_i-1}]} \left[\left(u'(t+1) - \frac{u''(t+1)}{u'(t+1)} \theta \eta_{t+1} q_{t+1} - u''(t+1) \sum_i \delta_{i,t+1} \phi_{i,t+1} \right) \right. \\ \left. ((\alpha + \xi_i) z_{i,t+1} k_{i,t+1}^{\alpha+\xi_i-1} - \phi_{i,t+1}^1) + \sum_i \delta_{i,t} \Omega_{i,t+1}^K \right. \\ \left. - u'(t)(q_{t+1} - \phi_{i,t}^1) - \theta \eta_{t+1} q_{t+1} \right] \\ + \frac{1}{\beta \mathbb{E}_t[\alpha z_{i,t+1} k_{i,t+1}^{\alpha+\xi_i-1}]} \left(u'(t) q_t + \Xi + \phi_{i,t}^2 u''(t) \sum_i \delta_{i,t} \phi_{i,t}^2 \right) \quad (40)$$

I prove the proposition by showing that the decentralized equilibrium with the taxes yields the same optimality conditions as the planner's constrained-efficient equilibrium. The constrained efficient equilibrium can be characterized by sequences $\{c_t, k_{t+1}, b_{t+1}, q_t, \lambda_t^*, \eta_t\}_{t=0}^\infty$ that satisfy equations (11), (12) (13), (21), (22), (24), (25), $k_t = 1$ together with the complementary slackness conditions. The regulated decentralized equilibrium is characterized by sequences $\{c_t, k_{t+1}, b_{t+1}, q_t, \lambda_t^* \eta_t\}_{t=0}^\infty$ that satisfy equations (10), (11), (12) (13), $k_t = 1$ together with the complementary slackness conditions. Substitution the expression for the debt tax (39) and (26) yields condition (24)) and identical conditions characterizing the two equilibria. Likewise, substituting the expression for the capital tax (40) and (25) yields

condition (23)) and identical conditions characterizing the two equilibria.

B.3 Solution algorithm

Following Bianchi and Mendoza (2018), I use a time iteration algorithm, modified to address the occasionally binding endogenous constraint and the additional number of state variables due to the multi-industry setting. Formally, the computation of the competitive equilibrium requires solving for functions

$\{\mathcal{B}(b, \mathcal{K}, \mathcal{Z}), \mathcal{Q}(b, \mathcal{K}, \mathcal{Z}), \mathcal{C}(b, \mathcal{K}, \mathcal{Z}), \mathcal{K}_i(b, \mathcal{K}, \mathcal{Z}), \eta(b, \mathcal{K}, \mathcal{Z})\}$ such that:

$$\mathcal{C}(b, \mathcal{K}, \mathcal{Z}) + \frac{\mathcal{B}(b, \mathcal{K}, \mathcal{Z})}{R} = \sum_i (z_i f(\mathcal{K}_i(b, \mathcal{K}, \mathcal{Z})) - \Phi_i(.)) + b \quad (41)$$

$$-\frac{\mathcal{B}(b, \mathcal{K}, \mathcal{Z})}{R} \leq \theta \mathcal{Q}(b, \mathcal{K}, \mathcal{Z}) \quad (42)$$

$$u'(\mathcal{C}(b, \mathcal{K}, \mathcal{Z})) = \beta R \mathbb{E}[u'(\mathcal{C}(\mathcal{B}(b, \mathcal{K}_i(b, \mathcal{K}, \mathcal{Z}), \mathcal{Z}'))] + \eta(b, \mathcal{K}, \mathcal{Z}) \quad (43)$$

$$\begin{aligned} u'(c)(q + \phi_i^2(.)) &= \beta \mathbb{E}[u'(\mathcal{C}(\mathcal{B}(b, \mathcal{K}_i(b, \mathcal{K}, \mathcal{Z}), \mathcal{Z}'))(\mathcal{Q}(b, \mathcal{K}, \mathcal{Z}) + z'_i f'(\mathcal{K}_i(b, \mathcal{K}, \mathcal{Z}))) \\ &\quad - \phi_i^1(.)) + \theta \mathcal{Q}(b, \mathcal{K}, \mathcal{Z}) \eta(b, \mathcal{K}, \mathcal{Z})] \quad \forall i = \{1, \dots, I\} \end{aligned} \quad (44)$$

The algorithm follows these steps:

1. Generate a discrete grid for the economy's bond position $G_b = \{b_1, \dots, b_M\}$, the capital allocation $G_{k_i} = \{k_1, \dots, k_M\}$ and the shock state space $G_{z_i} = \{z_1, \dots, z_M\}$. in addition, generate a discrete grid for the economy's relative position of current levels of relative productivities $G_{\Lambda_i} = \{\Lambda_1, \dots, \Lambda_M\}$. Choose an I use a piecewise linear function approximation and uniformly spaced grids.
2. Conjecture $\{\mathcal{B}_j(b, \mathcal{K}, \mathcal{Z}), \mathcal{Q}_j(b, \mathcal{K}, \mathcal{Z}), \mathcal{C}_j(b, \mathcal{K}, \mathcal{Z}), \mathcal{K}_{i,j}(b, \mathcal{K}, \mathcal{Z}), \eta_j(b, \mathcal{K}, \mathcal{Z})\}$
3. Set $l = 1$.
4. Solve for the values of $\{\mathcal{B}_{j-l}(b, \mathcal{K}, \mathcal{Z}), \mathcal{Q}_{j-l}(b, \mathcal{K}, \mathcal{Z}), \mathcal{C}_{j-l}(b, \mathcal{K}, \mathcal{Z}), \mathcal{K}_{i,j-l}(b, \mathcal{K}, \mathcal{Z}), \eta_{j-l}(b, \mathcal{K}, \mathcal{Z})\}$ at time $j - l$ functions above across all grids.
 - (a) Solve for the capital allocation combining the capital Euler equations and the market clearing condition into no-arbitrage conditions and using a root finding algorithm.

- (b) Assume the collateral constraint is not binding. Set $\eta_{j-l}(b, \mathcal{K}, \mathcal{Z}) = 0$ and solve for $\mathcal{B}_j(b, \mathcal{K}, \mathcal{Z})$ and $\mathcal{C}_j(b, \mathcal{K}, \mathcal{Z})$ using the FOCs.
 - (c) Check whether $-\frac{\mathcal{B}(b, \mathcal{K}, \mathcal{Z})}{R} \leq \theta \mathcal{Q}(b, \mathcal{K}, \mathcal{Z})$ holds using the asset price from the previous iteration to ensure stability.
 - (d) If the constraint is satisfied, move to the next grid point.
 - (e) Otherwise, solve for $\eta_{j-l}(b, \mathcal{K}, \mathcal{Z})$ with equality.
 - (f) Solve for $\mathcal{Q}_j(b, \mathcal{K}, \mathcal{Z})$.
5. Evaluate convergence error and iterate until convergence.